Cosmological domain walls from the breaking of S_4 flavor symmetry

Adil Jueid,[1,†] Mohamed Amin Loualidi[ORCID],[2,‡] Salah Nasri[ORCID],[2,3,*] and Mohamed Amine Ouahid[4,§]

[1]*Particle Theory and Cosmology Group, Center for Theoretical Physics of the Universe,*
Institute for Basic Science (IBS), 34126 Daejeon, South Korea
[2]*Department of physics, United Arab Emirates University, Al-Ain, United Arab Emirates*
[3]*The Abdus Salam International Centre for Theoretical Physics, Strada Costiera 11, I-34014 Trieste, Italy*
[4]*LPHE-Modeling and Simulations, Faculty of Science, Mohammed V University in Rabat,*
Morocco and Centre of Physics and Mathematics, Morocco

In this work, we delve into the often overlooked cosmological implications of the spontaneous breaking of the non-Abelian discrete groups, specifically focusing on the formation of domain walls in the case of S_4 flavor symmetry. In particular, we investigate three interesting breaking patterns of the S_4 group and study the structure of the domain walls in the broken phase for three possible residual symmetries. The presentation of domain walls in the case of multiple vacua is usually complicated, which therefore implies that most of the analyses only approximate their presentation. Here, we propose a subtle way to represent the S_4 domain wall networks by presenting the vacua in each breaking pattern as vectors with their components corresponding to their coordinates in the flavon space. Then, through the properties of the obtained vectors, we find that the domain wall networks can be represented by Platonic or Archimedean solids where the vertices represent the degenerate vacua while the edges correspond to the domain walls that separate them. As an illustration, we propose a type-II seesaw model that is based on the S_4 flavor symmetry, and study its phenomenological implications on the neutrino sector. To solve the domain wall problem within this toy model, we consider an approach based on high-dimensional effective operators induced by gravity that explicitly break the structure of the induced vacua favoring one vacuum over the others.

I. INTRODUCTION

In the past two decades, non-Abelian discrete symmetries have become more prominent in flavor model building. This interest grew particularly following the observation of large leptonic mixing angles from various neutrino oscillation experiments (see Refs. [1–3] for updated global fits). Non-Abelian discrete groups are increasingly employed to tackle the flavor problem which is connected to the lack of a mechanism within the Standard Model (SM) that explains the mass hierarchies of the different fermions and their mixing. Nevertheless, in order to achieve realistic predictions for the fermion masses and mixing angles at low energies, it is imperative to break the non-Abelian group due to the fact that the charged leptons and the three massive neutrinos are inherently distinct in the symmetric phase of the underlying flavor group. This breaking takes place when scalar fields called flavons, which are singlets under the SM gauge group, acquire nonzero vacuum expectation values (VEVs) along specific directions within the flavon space. On the other hand, the spontaneous symmetry breaking (SSB) of discrete groups gives rise to multiple degenerate vacua separated by surfacelike topological defects referred to as domain walls (DWs) [4,5]. The number of the vacua and DWs depends on the order of the broken group. Generally, these multiple vacua can be understood as the constituents of a topologically nontrivial vacuum manifold, defined by disconnected points in space with the same energy [6]. Once the field responsible for SSB stabilizes at one of these points—no point is preferred over any other—it cannot transition to any of the remaining points [7]. The regions between the degenerate ground states represent the DWs which, if proven to be stable, are disfavored by cosmological observations. To illustrate why this is an issue, notice that DWs are expected to enter a regime of dynamical scaling such that the number of defects is constant per Hubble horizon [8–10]. In this scaling regime, we have the property $H^{-1} \sim L \sim R$ where H^{-1} is the Hubble radius, L is the distance between two neighboring walls and R is the

*Corresponding author: snasri@uaeu.ac.ae, salah.nasri@cern.ch
[†]adiljueid@ibs.re.kr
[‡]ma.loualidi@uaeu.ac.ae
[§]mohamedamine_ouahid@um5.ac.ma

wall curvature radius which is proportional to the cosmological expansion factor $a(t)$. The energy density of DWs in this regime scales as a^{-1}, decreasing more slowly than radiation and matter which scales as a^{-4} and a^{-3} respectively [4–6]. As a result, DWs could eventually dominate the Universe at small redshift which is disfavored by the current cosmological observations; this is known as the domain wall problem [4]. Indeed, Zel'dovich, Kobzarev and Okun pointed out that stable DWs would cause a fast expansion of the Universe dramatically affecting the formation of galaxies and reducing the production rates of light elements during primordial nucleosynthesis [4]. Moreover, the presence of the walls in the current Universe would create unacceptable distortions in the cosmic microwave background (CMB) radiation that would violate the present limits on its homogeneity and isotropy [7].

Many approaches have been suggested to deal with the creation of DWs where the main idea is that they should either be unstable or remain subdominant until the present time. In particular, the energy scale associated with the SSB of the discrete groups should be low enough so that the energy density of the walls is a subdominant contribution to the total energy density of the Universe [11,12]. This scale is also restrained to be smaller that 1 MeV to prevent creating undesirable large anisotropies in the CMB [4]. Besides, the walls may exhibit instability if they manifest prior to the inflation era. However, below the inflationary scale, the most known solution to the DW problem was suggested by Zel'dovich *et al.* [4] where the DWs are unstable by assuming that the discrete symmetry is not exact. In other words, the introduction of explicit symmetry breaking terms create energy gaps between true and false vacua and in which case false vacua will fade before the walls dominate the energy density of the Universe (see also Refs. [5,6,13] for more details). The connection between the DW problem and flavor models that lead to it is usually overlooked in the literature. For instance, only the mechanism of DW creation and some of the solutions have been discussed in Refs. [14–21]. For instance, in Ref. [14] brief discussions exploring the explicit symmetry breaking solutions as well as a possibility that flat directions in the scalar potential acquire very large VEVs during inflation so that the DWs do not cause any problem is applied in the framework of the minimal supersymmetric standard model (MSSM) with an A_4 flavor group. Another example employing the A_4 group is proposed in Ref. [15] using a mechanism to stabilize the flavon potential with the desired alignment structure solves the DW problem independently of the scale of inflation. A similar approach is applied in the context of a supersymmetric S_4 flavor symmetry model in Ref. [16]. A different scenario is that the discrete flavor group is considered as an exact symmetry at the classical level and only broken at the quantum level by the QCD anomaly [22]. However, as demonstrated in [18] using A_4 and D_4 groups, QCD anomaly effects are

not enough to completely solve the DW problem since they cannot remove all the vacuum degeneracy. One more example with the alternating A_4 group is proposed in Ref. [20] in the context of the next-to-MSSM where the problem is solved by considering the explicit breaking of the discrete symmetry through the insertion of Planck-suppressed operators induced by supergravity.

In this work, we investigate for the *first time* the formation of DWs from the SSB of the flavor group S_4 within a nonsupersymmetric framework. Here, we emphasize on three S_4 breaking patterns that have been established as phenomenologically plausible, i.e., $S_4 \rightarrow Z_2 \times Z_2$, $S_4 \rightarrow Z_3$, and $S_4 \rightarrow Z_2$. Since for each of these patterns S_4 is only partially broken, the number of degenerate vacua is contingent upon the order of the broken subgroup of S_4.[1] For the above S_4 breaking patterns, the broken subgroups are given by the non-Abelian groups S_3, $\Sigma(8)$, and A_4, respectively. Therefore, the transformations among the vacua are characterized by non-Abelian structures making the representation of the vacuum manifold even more complicated. Here, we propose a subtle way to represent the S_4 DW networks by using the properties of the flavon space which is defined as a vector space that can accommodate all the dimensions of the S_4 irreducible representations.[2] After the SSB of S_4, the flavon field responsible for the breaking, say Ω, can be represented by a vector where its components correspond to its coordinates in the vector space. The remaining vectors (vacua) are obtained easily by applying the various elements of the broken subgroups of S_4 on $\langle \Omega \rangle$. Then, through the properties of the obtained vectors, we find that the DW networks can be represented by the Platonic or Archimedean solids where the vertices represent the degenerate vacua while the edges represent the domain walls. To address the DW problem and its possible solution in the case of the S_4 flavor group, we propose a toy model based on type-II seesaw mechanism which we confront to the recent neutrino data. The problem of DWs in this toy model is solved by introducing effective operators generated by gravity and suppressed by powers of the Planck mass which simply means that the S_4 symmetry is not exact after all.

The rest of this paper is organized as follows. In Sec. II, we start by identifying the S_4 breaking patterns consistent with the neutrino oscillation data. Then, we determine the breaking parts for each pattern, detailing properties crucial for DW formation. Finally, we offer a geometric description of DWs for each S_4 breaking pattern. In Sec. III, after

---

[1]In the context of Z_n Abelian groups, the vacuum manifold is composed of n degenerate vacua. The higher the order of the group, the greater the number of vacuum becomes leading to nontrivial DW networks.

[2]This is a vector space of dimension six where the first three components are reserved for S_4 triplets, the next two for S_4 doublets and the last for S_4 singlets.

exploring some well-known solutions to the DW problem, we build a toy model with S_4 flavor symmetry and examine neutrino phenomenology as well as propose a possible solution to the DW problem. We also qualitatively discuss the gravitational waves (GWs) arising from DWs in this toy model. We conclude in Sec. IV.

II. BREAKING OF S_4 SYMMETRY AND DOMAIN WALLS

In this section, we first specify the different S_4 symmetry breaking patterns that are known to be phenomenologically consistent with the neutrino oscillation data, and we define some notations for the irreducible representations of S_4 as well as its subgroups. Afterwards, we focus on identifying the broken parts for each breaking pattern and describe their properties relevant for the creation of domain walls. Finally, we provide a geometric description of the DWs generated for each S_4 breaking pattern.

A. Lepton residual symmetries from S_4

The breaking of non-Abelian discrete groups G_f is an essential part in the construction of flavor models to provide realistic predictions for lepton mixing angles. This breaking occurs when flavon fields acquire VEVs along specific directions in flavon space. Typically, the breaking of the flavor symmetry allows for the survival of different Abelian residual symmetries $G_{\rm res}$, which are subgroups of G_f. These residual symmetries give rise to distinct mixing patterns that can be explicitly derived by calculating the fermion mass matrices. Hence, the phenomenological viability of the fermion flavor structure is often assessed based on these surviving residual symmetries after the breaking of the underlying flavor group G_f. In this study, we examine the formation of DWs assuming S_4 as our flavor group, which breaks down into G_e and G_ν associated to the charged lepton and the neutrino sectors, respectively, and assuming that neutrinos are Majorana particles.

Depending on the flavon VEV alignment, the residual symmetry group corresponding to any one of the S_4 subgroups is illustrated in Fig. 1 where the residual symmetry group could be non-Abelian $\{A_4, D_4, S_3\}$ or Abelian $\{Z_4, Z_2 \times Z_2, Z_3, Z_2\}$. The breaking of S_4 down to one of its non-Abelian subgroups is excluded by current data since it leads to two degenerate neutrino mass states. For the case of Abelian subgroups, it is convenient to use the fact that S_4 is isomorphic to $G'_f = (Z_2 \times Z_2) \rtimes (Z_3 \rtimes Z_2)$, where $(Z_2 \times Z_2)$ refers to the Klein four-group denoted by K_4 in what follows, while $(Z_3 \rtimes Z_2)$ is isomorphic to the smallest non-Abelian group; the symmetric group S_3. Consequently, we can perceive S_4 as the semi-direct product of K_4 and S_3, denoted as $S_4 \cong K_4 \rtimes S_3$. This group contains 24 elements generated by three generators denoted by $\mathcal{S}, \mathcal{T}$, and $\mathcal{U}$. It is noteworthy, though, that only two generators are required to define S_4 [23]. However, in order to highlight the
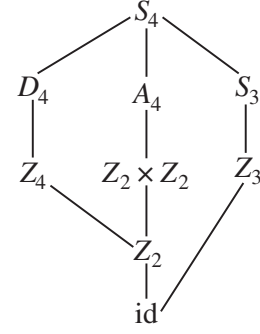

FIG. 1. Symmetry breaking patterns of S_4 discrete symmetry.

relationship between the alternating group A_4 and S_4, it is advantageous to choose the set of generators as $\mathcal{S}, \mathcal{T}$, and $\mathcal{U}$. By doing so, it becomes evident that $\mathcal{S}$ and $\mathcal{T}$ alone can generate the group A_4 [24]. Similarly, the two generators $\mathcal{T}$ and $\mathcal{U}$ alone can generate the group S_3 [25]. The S_4 group consists of five conjugacy classes and therefore contains five irreducible representations. These representations include two singlets $\mathbf{1}_{(1,1,1)}$ (trivial) and $\mathbf{1}'_{(1,1,-1)}$, one doublet $\mathbf{2}_{(2,-1,0)}$, and two triplets $\mathbf{3}_{(-1,0,-1)}$ and $\mathbf{3}'_{(-1,0,1)}$ with the indices referring to the characters of the generators $\mathcal{S}, \mathcal{T}$, and $\mathcal{U}$ respectively; see the Table II. In addition, S_4 has 20 Abelian subgroups, which consist of nine Z_2 subgroups, four Z_3 subgroups, three Z_4 subgroups, and four Klein-four subgroups (K_4). These symmetries can be expressed in terms of the S_4 generators as provided in Eq. (A3) of the Appendix.

Before going through the details of the S_4 breaking schemes, we would like to make the following comments relevant to the analysis of DWs formed under various S_4 breaking patterns:

(i) In this study, we adopt the representation matrices for the S_4 generators in the basis where $\mathcal{T}$ is diagonal [see Eq. (A2) in the Appendix]. This particular basis is commonly used in the literature since it leads to a diagonal charged-lepton mass matrix which remains invariant under $G_e = Z_3^{\mathcal{T}}$ generated by $\mathcal{T}$. Moreover, $G_e = Z_4$ is ruled out since it leads to values of the solar mixing angle outside 3σ range reported on by the authors of Ref. [26] while G_ν is either K_4 or Z_2 [27]. Consequently, Z_4 is discarded as a phenomenologically viable residual group.

(ii) One of our main interests is to search, for *the first time*, for graphical representations of the DW networks created during SSB of the S_4 group. Thus, we discuss the number of degenerate vacua extracted from the broken subgroups within each S_4 breaking pattern. In order to clarify this point from the beginning, consider the scenario of SSB of S_4 into one of its four Z_3 subgroups. In this case, the broken part corresponds to $K_4 \rtimes Z_2$, which is an order-8

structure that also represents the number of degenerate vacua, regardless of the specific Z_3's, K_4's and Z_2's subgroups of S_4 involved in this breaking pattern. For this reason, choosing one of the four Z_3's as the residual symmetry makes no difference for the study of the DWs. The same reasoning applies if the breaking pattern is into one of the nine Z_2 subgroups and/or the four K_4 subgroups of S_4.

(iii) The SSB of S_4 symmetry breaking can occur via a nontrivial S_4-singlet, an S_4-doublet, or an S_4-triplet whose VEVs preserve one of the subgroups of S_4. To simplify our discussion, we focus solely on the scenario where a flavon field is designated to transform as an S_4-triplet. However, we will provide additional comments whenever is necessary for the other cases.

(iv) The basis mentioned in the first comment is particularly interesting and useful for model building. However, in order to graphically represent the components that have undergone SSB, and thus to investigate the properties of DWs, we need to express the obtained degenerate vacua in a three-dimensional real basis. In this picture, $\mathcal{T}$ can be represented by a diagonal 3×3 matrix with eigenvalues $1, \omega$, and ω^2 and its typical eigenvectors x'_q are respectively given by

$$
\begin{aligned}
x'_1 &= x_1 + x_2 + x_3, \\
x'_2 &= x_1 + \omega^2 x_2 + \omega x_3, \\
x'_3 &= x_1 + \omega x_2 + \omega^2 x_3,
\end{aligned}
\tag{2.1}
$$

with x_1, x_2, and x_3 being the components of a complex vector space that defines the system basis for the triplet representation of S_4.

B. Symmetry breaking patterns of S_4

In view of the above, we will examine three breaking patterns of S_4 that are phenomenologically viable. Our study does not require the identification of the residual group between G_e and G_ν. Therefore, we do not specify here the sector within which S_4 breaking takes place but only later when we introduce the toy model that requires the definition of the scale at which S_4 is broken. References [26,28] explore all the possible combinations of the pairs G_e and G_ν. Let us now establish the S_4 breaking patterns within the basis provided in Eq. (A2):

(a) $\mathbf{S_4 \to K_4}$: Assuming that the residual K_4 symmetry is generated by $\{\mathcal{S}, \mathcal{U}\}$, this breaking can be realized by the S_4 triplet $\Phi' \equiv \mathbf{3}'_{(-1,0,1)}$ acquiring a VEV along the direction $\langle\Phi'\rangle = v_\Phi(1,1,1)^T$. Here, we should be careful about the generator of the third Z_2 group in G'_f—besides $K_4 \cong (Z_2^\mathcal{S} \times Z_2^\mathcal{U})$—given that its

generator should be broken in order for K_4 to be the only residual group.[3] For this reason, we consider that the third cyclic group $Z_2 \subset G'_f$ is generated by $\mathcal{T}^2\mathcal{S}\mathcal{T}$ which is the generator of one of the nine Z_2 subgroups of S_4 [see Eq. (A3)]. By exhibiting this breaking using the matrix representations of the generators of S_4 shown in Eq. (A2), we find

$$
\begin{aligned}
\mathcal{S}\langle\Phi'\rangle &= \langle\Phi'\rangle, & \mathcal{U}\langle\Phi'\rangle &= \langle\Phi'\rangle, \\
\mathcal{T}\langle\Phi'\rangle &\neq \langle\Phi'\rangle, & \mathcal{T}^2\mathcal{S}\mathcal{T}\langle\Phi'\rangle &\neq \langle\Phi'\rangle.
\end{aligned}
\tag{2.2}
$$

It is clear from this equation that the only preserved symmetry is $K_4 \cong (Z_2^\mathcal{S} \times Z_2^\mathcal{U})$ while the broken part is given by the symmetric group $S_3 \cong Z_3^\mathcal{T} \rtimes Z_2^{\mathcal{T}^2\mathcal{S}\mathcal{T}}$. In the case of the S_4 doublet $\mathbf{2}_{(2,-1,0)}$, it is not possible to exclusively decompose S_4 into $K_4^{\{\mathcal{S},\mathcal{U}\}}$. This is due to the fact that $Z_2^{\mathcal{T}^2\mathcal{S}\mathcal{T}}$ is always conserved, as $\mathcal{T}^2\mathcal{S}\mathcal{T}$ essentially represents a two-dimensional identity matrix. Consequently, regardless of the direction of any VEV, its application will yield an identical VEV direction. On the other hand, it is not possible to use the nontrivial singlet $\mathbf{1}'_{(1,1,-1)}$ for this breaking because it transforms oppositely under the $\mathcal{S}$ and $\mathcal{U}$ generators [see Eq. (A2) in the Appendix for more details]. It is important to emphasize that all the details regarding the VEV alignments described above depend on the choice of generators for all the groups involved in G'_f. For example, if we take a different Z_3 group in the breaking pattern $S_4 \to Z_3$ than $Z_3^\mathcal{T}$ we may need a different VEV structure for the flavon triplet than the one chosen above to realize this breaking.[4] Therefore, for different choices of the S_4 subgroups we may end up with different scalar sectors. However, this is completely model independent when it comes to the geometrical interpretation of the DWs created during each breaking pattern as we mentioned in the second comment above.

(b) $\mathbf{S_4 \to Z_3}$: Let us take the isomorphic group to be $G'_f \simeq (Z_2^\mathcal{S} \times Z_2^\mathcal{U}) \rtimes (Z_3^\mathcal{T} \rtimes Z_2^{\mathcal{T}\mathcal{S}\mathcal{T}^2})$, which means that the residual symmetry in this case is given by $Z_3^\mathcal{T}$. As a result, this breaking can be realized by the S_4 triplet $\Phi \equiv \mathbf{3}_{(-1,0,-1)}$ acquiring a VEV along the direction $\langle\Phi\rangle = v_\Phi(1,0,0)^T$ [29]. By exhibiting this breaking using the matrix representations of the generators of S_4 in Eq. (A2), we obtain

$$
\begin{aligned}
\mathcal{S}\langle\Phi\rangle &\neq \langle\Phi\rangle, & \mathcal{U}\langle\Phi\rangle &\neq \langle\Phi\rangle, \\
\mathcal{T}\langle\Phi\rangle &= \langle\Phi\rangle, & \mathcal{T}\mathcal{S}\mathcal{T}^2\langle\Phi\rangle &\neq \langle\Phi\rangle.
\end{aligned}
\tag{2.3}
$$

---

[3]The superscripts denote the generators for each Z_2 cyclic group.

[4]The other choices for the breaking pattern $S_4 \to Z_3$ are $Z_3^{\mathcal{S}\mathcal{T}}$, $Z_3^{\mathcal{T}\mathcal{S}}$, and $Z_3^{\mathcal{S}\mathcal{T}\mathcal{S}}$.

It is clear from this equation that the only preserved symmetry is Z_3^T while the broken part is given by $\Sigma(8) \equiv (Z_2^S \times Z_2^U) \rtimes Z_2^{TST^2}$ which is isomorphic to the dihedral D_4 group [30]. Notice by the way that if we use the other S_4 triplet $\mathbf{3}'_{(-1,0,1)}$ with the same VEV structure, the S_4 group will break down to $Z_2^U \rtimes Z_3^T$ which is isomorphic to the symmetric S_3 group. Consequently, the breaking pattern $S_4 \longrightarrow Z_3^T$ is not achieved with the triplet $\mathbf{3}'_{(-1,0,1)}$ unless a different VEV structure is chosen. We must stress out that the S_4 triplet $\Phi \equiv \mathbf{3}_{(-1,0,-1)}$ have to acquire a VEV along the direction $\langle \Phi \rangle = v_\Phi(-1,2,2)^T$ if we need to realize the breaking pattern $S_4 \rightarrow Z_3$ in the case where the residual group is represented by Z_3^{STS}. For the S_4 doublet $\mathbf{2}_{(2,-1,0)}$, there are no trivial VEV structures that allows the preservation of the T or STS generators, while the concluding remark for the S_4 singlet $\mathbf{1}'_{(1,1,-1)}$ in the previous breaking scheme holds as well for the S_4 breaking down to Z_3.

(c) $\mathbf{S_4} \longrightarrow \mathbf{Z_2}$: let us denote the three Z_2 replicas in the isomorphic group $G'_f \simeq (Z_2 \times Z_2) \rtimes (Z_3 \rtimes Z_2)$ by Z_2^U, Z_2^S, and Z_2^{SU} where we take the latter as the residual symmetry associated with the semidirect product $(Z_3 \rtimes Z_2)$. Assuming that this breaking is induced by the S_4 triplet $\Phi \equiv \mathbf{3}_{(-1,0,-1)}$, the VEV alignment in this case is given by $\langle \Phi \rangle = v_\Phi(2,-1,-1)^T$ as shown in Ref. [29]. This can be easily exhibited using the matrix representations of the generators of S_4, given in Eq. (A2), as follows:

$$S\langle\Phi\rangle \neq \langle\Phi\rangle, \qquad U\langle\Phi\rangle \neq \langle\Phi\rangle,$$
$$T\langle\Phi\rangle \neq \langle\Phi\rangle, \qquad SU\langle\Phi\rangle = \langle\Phi\rangle. \qquad (2.4)$$

It is clear from this equation that the only preserved symmetry is Z_2^{SU} while the broken part is given by $Z_2^U \times Z_2^S \rtimes Z_3^T$ which is isomorphic to the alternating A_4 group. It is worth noticing that the use of the other S_4 triplet $\mathbf{3}'_{(-1,0,1)}$ while maintaining the same VEV structure leads to the breakdown of the S_4 group into its Z_2 subgroup generated by U where it is straightforward to verify that $U\langle\Phi\rangle = \langle\Phi\rangle$. On the other hand, thinking of Z_2^{SU} as one of the Z_2 groups in the Klein four group leads to the broken part $Z_2^U \rtimes Z_2^S \rtimes Z_3^T$ which is a different group compared to $Z_2^U \times Z_2^S \rtimes Z_3^T$. However, both of these groups have the same order, thereby resulting in an equal number of degenerate vacua, as mentioned in the second comment provided above. We will now take a brief look at alternative representations of flavons. If we examine the breaking pattern $S_4 \longrightarrow Z_2$ via an S_4 doublet $\mathbf{2}_{(2,-1,0)}$, the residual Z_2 symmetry generated by SU is no longer a viable choice. This is because SU and U transform

in the same manner, leading to the same outcome when applied to $\langle\Phi\rangle$. However, if we designate the residual symmetry as Z_2^S, we can achieve this breaking pattern by adopting a VEV configuration as $\langle\Phi\rangle = v_\Phi(1,0)^T$. Another possibility is to opt for different $Z_2 \in G'_f$ subgroups among the nine available in S_4. On the other hand, it is not possible to use the nontrivial singlet $\mathbf{1}'_{(1,1,-1)}$ for this breaking because it transforms in the same manner under S and T generators and thus the T generator will be always preserved together with S. As a result, the nontrivial singlet will inevitably cause the breakdown of S_4 to a subgroup other than Z_2.

C. DWs configuration

1. Introduction

To understand how DWs are positioned in flavon space, it is advantageous to look for concrete visual representations. These representations aid in illustrating the outcomes of symmetry breaking, ultimately facilitating the understanding of the connections among distinct regions that interpolate between the various Φ_a-vacua. In particular, we are going to show that the use of networks or graphical representations to present DWs arising from the SSB of the S_4 group can be useful to capture the properties of these topological defect, such as their boundaries, intersections, and connectivity. Moreover, these graphical representations may also be interpreted as quiver diagrams in the flavon space; denoted in what follows by ζ.

To establish a comprehensive framework for the S_4 group's flavon space, our approach involves envisioning a six-dimensional vector space $\mathbf{V}$ capable of accommodating the various dimensions associated with S_4 irreducible representations. Specifically, we represent this vector as $\mathbf{V} = (x_1, x_2, x_3, x_4, x_5, x_6) \in \mathbb{C}^6$. As mentioned in the previous section, our primary focus lies on S_4 triplets, leading us to conceive the flavon triplet $\mathbf{\Phi}$ in terms of the vector space $\mathbf{V}$ components as[5]

$$\mathbf{\Phi} \sim \Phi_j x_j, \quad j = 1, 2, 3. \qquad (2.5)$$

On the other hand, in order to use real graphical representation for DWs, we need to find a real representation for the flavon fields which are in general complex fields. We can approach this by considering the splitting of the flavon

---

[5]A more general scenario would be to consider a collective flavon field $F \sim F_i x_i$, where $F = (\mathbf{\Phi}, \varphi, \sigma)$ with $\varphi = \varphi_k x_k$, $k = 4, 5$ being a flavon doublet while $\sigma = \sigma x_6$ is a flavon singlet. As a result, we can think of these x'_is as the foundation of a vector basis system in a flavon space ζ where the first three directions (x_1, x_2, x_3) correspond to the S_4-triplets, the subsequent two directions (x_4, x_5) correspond to the S_4-doublets and the last direction x_6 corresponds to S_4-singlets.

fields as well as the vector space **V** into real and imaginary parts,

$$\Phi_j = \Re(\Phi_j) + i\Im(\Phi_j),$$
$$\mathbf{V}_j = \Re(U_j) + i\Im(R_j), \quad j = 1, 2, 3, \qquad (2.6)$$

where U_j and R_j are real 3D vectors that can be understood as the constituents of x_j as $x_1 = (U_1, R_1)^T, \ldots, x_3 = (U_3, R_3)^T$. With this real representation, we can think of the complex 3D expansion $\boldsymbol{\Phi} \sim \Phi_j x_j$ as a real six-dimensional vector like,

$$\boldsymbol{\Phi} \sim \sum_j [\Re(\boldsymbol{\Phi}_j)U_j + \Im(\boldsymbol{\Phi}_j)R_j] \in \mathbb{R}. \qquad (2.7)$$

For illustration, we demonstrated in the previous section that the $S_4 \to K_4$ symmetry breaking pattern can be achieved through a flavon triplet Φ' which attains a VEV along the direction $\langle \Phi' \rangle = v_{\Phi'}(1, 1, 1)^T$. This particular VEV can be expressed in the real six-dimensional basis as

$$\langle \Phi' \rangle = v_{\Phi}(1, 0, 1, 0, 1, 0)^T. \qquad (2.8)$$

Expanding upon this, there exists another VEV direction involving complex entries that corresponds to the $S_4 \to K_4$ breaking pattern. We label this direction as $\langle \Phi'' \rangle = v_{\Phi''}(1, \omega, \omega^2)^T$ where $\omega = -1/2 + i\sqrt{3}/2$ [29]. In this case, $\langle \Phi'' \rangle$ is represented in the real basis as

$$\langle \Phi'' \rangle = v_{\Phi''}(1, 0, -1/2, \sqrt{3}/2, -1/2, -\sqrt{3}/2)^T. \qquad (2.9)$$

From a geometric perspective, the VEV $\langle \Phi' \rangle$ responsible for the breaking can be represented by a vector situated in one of the real directions within the vector space (U_k, R_k). The components of this vector correspond to its coordinates within that space. Then, the transformations applied to $\langle \Phi' \rangle$ by the various elements of the S_4 group create a polygon in the space defined by (U_k, R_k). The number of vertices in the polygon is equal to the number of degenerate vacua resulting from the SSB of the S_4 group. For example, when the S_4 group is completely broken, the VEV responsible for this breaking, say $\langle \Omega \rangle$, splits into 24 vacua with the same energy $\langle \Omega \rangle_i \equiv \epsilon_i$ with $i = 1, \ldots, 24$. Among these vacua, one is just the VEV used to break S_4; say $\epsilon_1 = \langle \Omega \rangle$. The remaining 23 vacua emerge through the application of the S_4 group elements upon ϵ_1. These transformations generate a polygon with the following 24 vertices

$$\epsilon_1 = \langle \Omega \rangle, \quad \epsilon_2 = \mathcal{S}\epsilon_1, \quad \epsilon_3 = \mathcal{T}\mathcal{S}\mathcal{T}^2\epsilon_1, \quad \epsilon_4 = \mathcal{T}^2\mathcal{S}\mathcal{T}\epsilon_1, \quad \epsilon_5 = \mathcal{U}\epsilon_1, \quad \epsilon_6 = \mathcal{T}\mathcal{U}\epsilon_1$$

$$\epsilon_7 = \mathcal{S}\mathcal{U}\epsilon_1, \quad \epsilon_8 = \mathcal{T}^2\mathcal{U}\epsilon_1, \quad \epsilon_9 = \mathcal{S}\mathcal{T}\mathcal{S}\mathcal{U}\epsilon_1, \quad \epsilon_{10} = \mathcal{S}\mathcal{T}^2\mathcal{S}\mathcal{U}\epsilon_1, \quad \epsilon_{11} = \mathcal{T}\epsilon_1, \quad \epsilon_{12} = \mathcal{S}\mathcal{T}\epsilon_1$$

$$\epsilon_{13} = \mathcal{T}\mathcal{S}\epsilon_1, \quad \epsilon_{14} = \mathcal{S}\mathcal{T}\mathcal{S}\epsilon_1, \quad \epsilon_{15} = \mathcal{T}^2\epsilon_1, \quad \epsilon_{16} = \mathcal{S}\mathcal{T}^2\epsilon_1, \quad \epsilon_{17} = \mathcal{T}^2\mathcal{S}\epsilon_1, \quad \epsilon_{18} = \mathcal{S}\mathcal{T}^2\mathcal{S}\epsilon_1$$

$$\epsilon_{19} = \mathcal{S}\mathcal{T}\mathcal{U}\epsilon_1, \quad \epsilon_{20} = \mathcal{T}\mathcal{S}\mathcal{U}\epsilon_1, \quad \epsilon_{21} = \mathcal{T}^2\mathcal{S}\mathcal{U}\epsilon_1, \quad \epsilon_{22} = \mathcal{S}\mathcal{T}^2\mathcal{U}\epsilon_1, \quad \epsilon_{23} = \mathcal{T}\mathcal{S}\mathcal{T}^2\mathcal{U}\epsilon_1, \quad \epsilon_{24} = \mathcal{T}^2\mathcal{S}\mathcal{T}\mathcal{U}\epsilon_1, \qquad (2.10)$$

where the elements of S_4 are provided in the Appendix. The obtained polygonal graph can be interpreted as a DW quiver observed from the flavon space ζ, where S_4 is completely broken. On the other hand, we mentioned in the previous section that the models that are phenomenologically viable for explaining the observed flavor structure correspond to partial breaking of S_4 down to one of its subgroups; Z_2, Z_3, or K_4. Therefore, the broken parts in each of these breaking scenarios will yield a reduced number of vertices compared to the scenario where S_4 is completely broken. In what follows, we will examine each case independently, with the aim of describing the DW properties by identifying the polygonal graphs associated with each breaking pattern.

2. DWs for $S_4 \to K_4$ breaking

As outlined above, the breaking pattern $S_4 \to K_4$ can be realized by the flavon triplet $\Phi' \equiv 3'_{(-1,0,1)}$ acquiring a VEV along the direction $\langle \Phi' \rangle = v_{\Phi}(1, 1, 1)^T$. The Klein four

group we have chosen for this study is $K_4 \cong Z_2^{\mathcal{S}} \times Z_2^{\mathcal{U}}$ and thus, this breaking can be expressed using G'_f as follows:

$$Z_2^{\mathcal{S}} \times Z_2^{\mathcal{U}} \rtimes Z_3^{\mathcal{T}} \rtimes Z_2^{\mathcal{T}^2\mathcal{S}\mathcal{T}} \xrightarrow{\langle \Phi' \rangle} K_4, \qquad (2.11)$$

where the broken part is given by $Z_3^{\mathcal{T}} \rtimes Z_2^{\mathcal{T}^2\mathcal{S}\mathcal{T}}$ which is isomorphic to the symmetric group S_3. The order of S_3 is six which means that the initial S_4 invariant vacuum gets now split into six vacua with the same energy $\langle \Phi' \rangle_i \equiv \varphi'_i$ with $i = 1, \ldots, 6$. These six vacua are positioned within the flavon space ζ and collectively establish the vertices of a Platonic solid known as a regular octahedron as depicted in Fig. 2. One of the vertices defining the octahedron is the K_4- invariant vacuum used for the $S_4 \to K_4$ breaking; $\varphi'_1 = \langle \Phi' \rangle$. To derive the remaining five φ'_i vacua, we act upon φ'_1 with the generators of $Z_3^{\mathcal{T}} \rtimes Z_2^{\mathcal{T}^2\mathcal{S}\mathcal{T}}$ as follows:
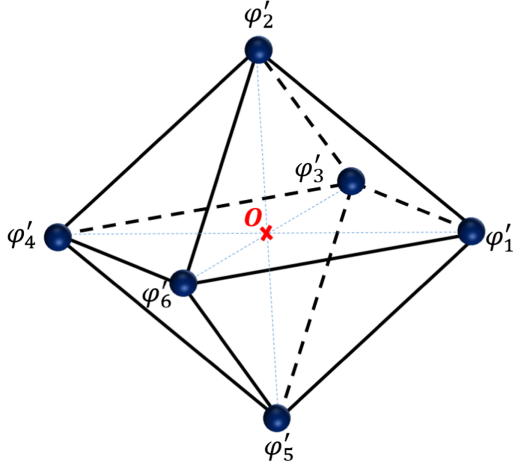
FIG. 2. A regular octahedron viewed from the flavon space ζ. The six vertices represent the six degenerate vacua, while the edges that connect them stand for domain walls.

$$\varphi_1' = \langle \Phi' \rangle, \qquad \varphi_2' = \mathcal{T}\varphi_1',$$
$$\varphi_3' = \mathcal{T}^2\varphi_1', \qquad \varphi_4' = \mathcal{T}^2\mathcal{S}\mathcal{T}\varphi_1',$$
$$\varphi_5' = \mathcal{T}(\mathcal{T}^2\mathcal{S}\mathcal{T})\varphi_1', \qquad \varphi_6' = \mathcal{T}^2(\mathcal{T}^2\mathcal{S}\mathcal{T})\varphi_1'. \quad (2.12)$$

In the complex three-dimensional space $\mathbb{C}^3$, these transformations lead to

$$\varphi_{1,4}' = \pm v_{\Phi'} \begin{pmatrix} 1 \\ 1 \\ 1 \end{pmatrix}, \qquad \varphi_{2,5}' = \pm v_{\Phi'} \begin{pmatrix} 1 \\ \omega^2 \\ \omega \end{pmatrix},$$

$$\varphi_{3,6}' = \pm v_{\Phi'} \begin{pmatrix} 1 \\ \omega \\ \omega^2 \end{pmatrix}. \qquad (2.13)$$

In the real vector basis, we have to use real variables, so the dimensions of the above vectors has to be doubled $\mathbb{C}^3 \sim \mathbb{R}^6$. Applying the same procedure outlined in Eqs. (2.8) and (2.9), we find

$$\varphi_{1,4}' = \pm v_{\Phi'} \begin{pmatrix} 1 & 0 & 1 & 0 & 1 & 0 \end{pmatrix}^T,$$

$$\varphi_{2,5}' = \pm v_{\Phi'} \begin{pmatrix} 1 & 0 & -1/2 & -\sqrt{3}/2 & -1/2 & \sqrt{3}/2 \end{pmatrix}^T,$$

$$\varphi_{3,6}' = \pm v_{\Phi'} \begin{pmatrix} 1 & 0 & -1/2 & \sqrt{3}/2 & -1/2 & -\sqrt{3}/2 \end{pmatrix}^T,$$
$$(2.14)$$

where the modulus of each vector is given by $\sqrt{3}v_{\Phi'}$. These vectors satisfy a constraint such that $\sum_{i=6} \varphi_i' = 0$, defining a regular octahedron with six vertices, twelve edges, and eight faces. We need to emphasize that each vertex (vacuum state) of an octahedron has exactly four adjacent

vertices (connected by edges), and thus the DWs form between these adjacent vertices. For example, in Fig. 2, the vertex corresponding to the state φ_1' has four adjacent vertices denoted by φ_2', φ_3', φ_5', and φ_6'. Whereas the vertex corresponding to the vacuum state φ_4' positioned along the diagonal is not adjacent. Moreover, moving along the diagonal $\varphi_1'\varphi_4'$ involves passing through the octahedron's center, where the S_4 group remains unbroken ($v_{\Phi'} \to 0$), and thus no DWs are present. Notably, the broken part in this pattern corresponds to the non-Abelian group S_3. Therefore, we need to consider transformations of the entire S_3 group. Since the transition along the diagonal covers a larger distance in the flavon space compared to transitions between adjacent vertices [see Eq. (II.15)], the shift between φ_1' and φ_4' can be achieved in four different ways, for example, through all the adjacent vertices to φ_1'. For instance, we can have a transition through φ_6'. This can be realized using transformations such as $\varphi_6' = \mathcal{T}\mathcal{S}\mathcal{T}\varphi_1'$ and then $\varphi_4' = \mathcal{T}\varphi_6' = \mathcal{T}^2\mathcal{S}\mathcal{T}\varphi_1'$. Proving the properties of the octahedron using the six vacua in Eq. (2.14) is a straightforward task. To illustrate this, let us consider the fact that all the edges of an octahedron possess equal lengths. By examining the right triangular face defined by vertices φ_1', φ_2', and φ_3' as depicted in Fig. 2, we can deduce that $d_{12}' = d_{13}' = d_{23}' = \sqrt{6}v_{\Phi'}$, where $d_{12}' = \|\varphi_2' - \varphi_1'\|$, $d_{13}' = \|\varphi_3' - \varphi_1'\|$ and $d_{23}' = \|\varphi_3' - \varphi_2'\|$. Furthermore, all the diagonals within an octahedron share the same length. This fact becomes evident when we calculate the lengths of the three diagonals converging at the center of the octahedron. Thus, following the notations in Fig. 2, we find that

$$d_{14}' = d_{25}' = d_{36}' = 2\sqrt{3}v_{\Phi'}, \qquad (2.15)$$

where $d_{14}' = \|\varphi_4' - \varphi_1'\|$, $d_{25}' = \|\varphi_5' - \varphi_2'\|$ and $d_{36}' = \|\varphi_6' - \varphi_3'\|$.

3. DWs for $S_4 \to Z_3$ breaking

As mentioned in the previous subsection, the breaking pattern $S_4 \to Z_3$ is realized by the flavon triplet Φ acquiring its VEV along the direction $\langle \Phi \rangle = v_\Phi(1,0,0)^T$ and can be expressed using $G_f' = Z_2^S \times Z_2^U \rtimes Z_3^T \rtimes Z_2^{TST^2}$ as follows:

$$Z_2^S \times Z_2^U \rtimes Z_3^T \rtimes Z_2^{TST^2} \xrightarrow{\langle \Phi \rangle} Z_3^T, \qquad (2.16)$$

where the broken part is given by $\Sigma_8 = (Z_2^S \times Z_2^U) \rtimes Z_2^{TST^2}$. The order of Σ_8 is eight which means that the initial S_4 invariant vacuum gets now split into eight vacua with the same energy $\langle \Phi \rangle_i \equiv \varphi_i$ with $i = 1, \dots, 8$. These vacua are situated within the flavon space ζ and collectively establish the vertices of a regular cube, as depicted in Fig. 3. The process of determining the coordinates of these eight vacua is straightforward. We know that one of them is just the
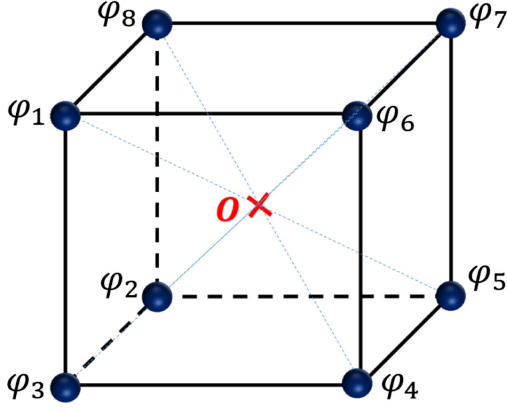
FIG. 3. A regular cube viewed from the flavon space ζ. The eight vertices represent the eight degenerate vacua, while the edges that connect them stand for domain walls.

Z_3^T-invariant vacuum used for the breaking of S_4 down to Z_3^T denoted by $\varphi_1 = \langle\Phi\rangle$. To derive the remaining seven φ_i vacua, we act upon φ_1 with the generators of Σ_8 by using the representation matrices of the S_4 generators provided in Eq. (A2) as follows:

$$
\begin{aligned}
\varphi_1 &= \langle\Phi\rangle, &\varphi_2 &= \mathcal{S}\varphi_1, \\
\varphi_3 &= \mathcal{S}\mathcal{U}(\mathcal{T}\mathcal{S}\mathcal{T}^2)\varphi_1, &\varphi_4 &= \mathcal{S}(\mathcal{T}\mathcal{S}\mathcal{T}^2)\varphi_1, \\
\varphi_5 &= \mathcal{U}\varphi_1, &\varphi_6 &= \mathcal{S}\mathcal{U}\varphi_1, \\
\varphi_7 &= \mathcal{T}\mathcal{S}\mathcal{T}^2\varphi_1, &\varphi_8 &= \mathcal{U}(\mathcal{T}\mathcal{S}\mathcal{T}^2)\varphi_1.
\end{aligned} \tag{2.17}
$$

This is expressed explicitly in the complex three-dimensional space $\mathbb{C}^3$ as follows:

$$
\varphi_{1,5} = \pm v_\Phi \begin{pmatrix} 1 \\ 0 \\ 0 \end{pmatrix}, \qquad \varphi_{2,6} = \pm\frac{v_\Phi}{3}\begin{pmatrix} -1 \\ 2 \\ 2 \end{pmatrix},
$$

$$
\varphi_{3,7} = \pm\frac{v_\Phi}{3}\begin{pmatrix} 1 \\ -2\omega^2 \\ -2\omega \end{pmatrix}, \qquad \varphi_{4,8} = \pm\frac{v_\Phi}{3}\begin{pmatrix} -1 \\ 2\omega \\ 2\omega^2 \end{pmatrix}. \tag{2.18}
$$

Being associated with Σ_8, these vacua are related to each other by $(Z_2^S \times Z_2^U)\rtimes Z_2^{\mathcal{T}\mathcal{S}\mathcal{T}^2}$ transformations. Applying the same procedure outlined in Eqs. (2.8) and (2.9), we find the following expressions for the direction in $\mathbb{R}^6$:

$$
\varphi_{1,5} = \pm v_\Phi \begin{pmatrix} 1 & 0 & 0 & 0 & 0 & 0 \end{pmatrix}^T,
$$

$$
\varphi_{2,6} = \pm\frac{v_\Phi}{3}\begin{pmatrix} -1 & 0 & 2 & 0 & 2 & 0 \end{pmatrix}^T,
$$

$$
\varphi_{3,7} = \pm\frac{v_\Phi}{3}\begin{pmatrix} 1 & 0 & 1 & \sqrt{3} & 1 & -\sqrt{3} \end{pmatrix}^T,
$$

$$
\varphi_{4,8} = \pm\frac{v_\Phi}{3}\begin{pmatrix} -1 & 0 & -1 & \sqrt{3} & -1 & -\sqrt{3} \end{pmatrix}^T, \tag{2.19}
$$

where the modulus of each vector is given by $\Re v_\Phi$. These vectors satisfy a constraint such that $\sum_{i=8}\varphi_i = 0$, defining a cube with eight vertices, 12 edges, and six faces. The diagonals of this cube converge at a unique point known as the center of symmetry, also referred to as the barycenter (or the core of the cube) of its eight vertices where the complete S_4 symmetry is manifest. Notably, it is straightforward to prove that connecting these eight vertices creates a cube, as confirmed by verifying that the 12 edges interconnecting the eight vertices in Fig. 3 are all of equal length. This equality can be easily calculated by fixing one vertex at a time. Given that we know that each vertex in a cube is connected to three edges, consider φ_1 in Fig. 3; it is connected via three edges to φ_3, φ_6, and φ_8. As a result, we find that

$$
d_{13} = d_{16} = d_{18} = \sqrt{\tfrac{4}{3}}v_\Phi, \text{ where } d_{13} = \|\varphi_3 - \varphi_1\|, \ d_{16} = \|\varphi_6 - \varphi_1\| \text{ and } d_{18} = \|\varphi_8 - \varphi_1\|.
$$

4. DWs for $S_4 \to Z_2$ breaking

As described previously, the breaking pattern $S_4 \to Z_2$ can be realized by the flavon triplet $\Phi \equiv 3_{(-1,0,-1)}$ acquiring a VEV along the direction $\langle\Phi\rangle = v_\Phi(2,-1,-1)^T$. This breaking can be expressed using G'_f as follows:

$$
Z_2^S \times Z_2^U \rtimes Z_3^T \rtimes Z_2^{SU} \xrightarrow{\langle\Phi\rangle} Z_2^{SU}, \tag{2.20}
$$

where the broken part is given by $Z_2^S \times Z_2^U\rtimes Z_3^T$ which is isomorphic to the alternating A_4 group of order 12. Therefore, the initial S_4 invariant vacuum gets now split into twelve vacua with same energy $\langle\Phi\rangle_i \equiv \phi_i$ with $i = 1, \ldots, 12$. These vacua are located within the flavon space ζ and collectively establish the vertices of an Archimedean solid known as cuboctahedron as depicted in Fig. 4. One of the vertices defining this solid is the Z_2^{SU}-invariant vacuum which we denote as $\phi_1 = \langle\Phi\rangle$. As in the previous cases, we act upon ϕ_1 with the generators of $Z_2^S \times Z_2^U \rtimes Z_3^T$ to derive the remaining twelve ϕ_i vacua,

$$
\begin{aligned}
\phi_1 &= \langle\Phi\rangle, &\phi_2 &= \mathcal{T}\phi_1, &\phi_3 &= \mathcal{T}^2\phi_1, \\
\phi_4 &= \mathcal{T}\mathcal{S}\mathcal{T}^2\phi_1, &\phi_5 &= \mathcal{S}\mathcal{T}^2\mathcal{S}\phi_1, &\phi_6 &= \mathcal{S}\mathcal{T}\mathcal{S}\phi_1, \\
\phi_7 &= \mathcal{U}\phi_1, &\phi_8 &= \mathcal{T}\mathcal{U}\phi_1, &\phi_9 &= \mathcal{T}^2\mathcal{U}\phi_1, \\
\phi_{10} &= \mathcal{T}\mathcal{S}\mathcal{T}^2\mathcal{U}\phi_1, &\phi_{11} &= \mathcal{S}\mathcal{T}^2\mathcal{S}\mathcal{U}\phi_1, &\phi_{12} &= \mathcal{S}\mathcal{T}\mathcal{S}\mathcal{U}\phi_1.
\end{aligned} \tag{2.21}
$$

In the complex three-dimensional space $\mathbb{C}^3$, these transformations lead to

$$
\phi_{1,7} = \pm v_\Phi \begin{pmatrix} 2 \\ -1 \\ -1 \end{pmatrix}, \qquad
\phi_{2,8} = \pm v_\Phi \begin{pmatrix} 2 \\ -\omega^2 \\ -\omega \end{pmatrix}, \qquad
\phi_{3,9} = \pm v_\Phi \begin{pmatrix} 2 \\ -\omega \\ -\omega^2 \end{pmatrix},
$$

$$
\phi_{4,10} = \pm v_\Phi \begin{pmatrix} 0 \\ \omega^2 - \omega \\ -\omega^2 + \omega \end{pmatrix}, \qquad
\phi_{5,11} = \pm v_\Phi \begin{pmatrix} 0 \\ \omega^2 - 1 \\ \omega - 1 \end{pmatrix}, \qquad
\phi_{6,12} = \pm v_\Phi \begin{pmatrix} 0 \\ \omega - 1 \\ \omega^2 - 1 \end{pmatrix}. \tag{2.22}
$$

Applying the same procedure outlined in Eqs. (2.8) and (2.9), we find

$$
\phi_{1,7} = \pm v_\Phi \begin{pmatrix} 2 & 0 & -1 & 0 & -1 & 0 \end{pmatrix}^T, \qquad
\phi_{2,8} = \pm v_\Phi \begin{pmatrix} 2 & 0 & 1/2 & \sqrt{3}/2 & 1/2 & -\sqrt{3}/2 \end{pmatrix}^T,
$$

$$
\phi_{3,9} = \pm v_\Phi \begin{pmatrix} 2 & 0 & 1/2 & -\sqrt{3}/2 & 1/2 & \sqrt{3}/2 \end{pmatrix}^T, \qquad
\phi_{4,10} = \pm v_\Phi \begin{pmatrix} 0 & 0 & 0 & -\sqrt{3} & 0 & \sqrt{3} \end{pmatrix}^T,
$$

$$
\phi_{5,11} = \pm v_\Phi \begin{pmatrix} 0 & 0 & -3/2 & -\sqrt{3}/2 & -3/2 & \sqrt{3}/2 \end{pmatrix}^T, \qquad
\phi_{6,12} = \pm v_\Phi \begin{pmatrix} 0 & 0 & -3/2 & \sqrt{3}/2 & -3/2 & -\sqrt{3}/2 \end{pmatrix}^T, \tag{2.23}
$$

where the modulus of each vector is given by $\sqrt{6}v_\Phi$. These vectors satisfy a constraint such that $\sum_{i=12} \phi_i = 0$, defining a regular cuboctahedron with 12 vertices, 24 edges, and 14 faces (six square faces and eight triangular faces). The properties of the regular cuboctahedron are easily verified through the real vectors in Eq. (2.23). For example, we know that all the edges in this Fig. (4) are of equal length which we can verify by calculating, for instance, the distances between the edges of the square face $\phi_1\phi_3\phi_4\phi_5$ where we find that $d_{13} = d_{34} = d_{45} = d_{51} = \sqrt{6}v_\Phi$ where $d_{ij} = \|\phi_i - \phi_j\|$.

To summarize, our strategy for representing DW networks in a real Euclidean space has led to the derivation of Platonic and Archimedean solids. In this visual framework, the vertices represent the degenerate vacua corresponding to each S_4 breaking pattern, while the edges represent
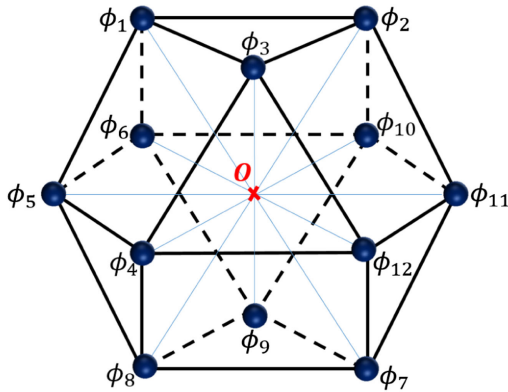
the DWs. Consequently, these graphical depictions not only enhance our intuitive comprehension of the vacuum structure but also facilitate the accurate determination of the number of DWs associated with each S_4 breaking pattern. Notably, examining transformations among the degenerate vacua for each S_4 breaking pattern reveals that no DWs emerge between the diagonals of the provided Platonic and Archimedean solids. On the other hand, to investigate the characteristics of these DWs, an examination of the scalar potential associated with the scalars responsible for S_4 breaking is necessary. An essential component of this involves estimating the dimensions, including both the width and the surface area, of these DWs using a spacetime framework; see Sec. V A of Ref. [20] for the case of A_4 group.

III. A RESOLUTION FOR THE DW PROBLEM WITHIN A NEUTRINO TOY MODEL

In this section, we begin by reviewing some viable solutions to the DW problem and we use one of these solutions within a toy model that incorporates the S_4 flavor symmetry. Then, we analyze the neutrino phenomenology in this model, comment on the solution using high-dimensional operators and at the end we qualitatively discuss the GWs arising from DWs in this case.

A. Neutrino phenomenology

We illustrate the DW problem and its solution using a toy model that is based on the type-II seesaw mechanism with an S_4 flavor symmetry. In this study, we will focus solely on the neutrino sector and ignore the charged lepton sector. This is due to the fact that in minimal flavor models, the flavon fields cannot be used simultaneously in the neutrino and

FIG. 4. A regular cuboctahedron viewed from the flavon space ζ. The twelve vertices represent the twelve degenerate vacua, while the edges that connect them stand for domain walls.

TABLE I. $SU(2)_L$ and S_4 transformations of the particle content of the model.

Fields	L_{iL}	H	Δ	Φ	σ	ρ
$SU(2)_L$	2	2	3	1	1	1
S_4	**3**	**1**	**1'**	**3**	**2**	**1'**

charged lepton sectors while preserving the correct vacuum alignment [31,32]. Consequently, these two sectors are decoupled from each other, including the scalar potentials of the flavons used in both sectors. Usually, this is achieved by acquiring additional Z_N symmetries to control the model Lagrangian and prevent unwanted couplings. The particle content in this toy model consists of $L_{iL} = (\nu_{iL}, \ell_{iL})^T$, $H = (\phi^+, \phi^0)^T$, and $\Delta = (\Delta^{++}, \Delta^+, \Delta^0)^T$ with L_{iL}, H, and Δ being the lepton doublet, Higgs doublet and scalar triplet with hypercharges -1, 1, and 2, respectively. The scalar triplet is responsible for the generation of small neutrino masses through the type-II seesaw mechanism. In addition, we extend the particle content of the SM with three gauge singlet flavon fields (Φ, σ, ρ) to achieve the SSB of the S_4 symmetry and ensure a trimaximal mixing for the neutrino mass matrix. The transformations of these fields under $SU(2)_L \times S_4$ are summarized in Table I. By using these field transformations, the most general Lagrangian invariant under $SU(2)_L \times U(1)_Y \times S_4$ is given by

$$\mathcal{L} \equiv \frac{\lambda_\Phi}{\Lambda} \left(\bar{L}_{iL}^c i\sigma_2 \Delta L_{jL} \right) \Phi + \frac{\lambda_\sigma}{\Lambda} \left(\bar{L}_{iL}^c i\sigma_2 \Delta L_{jL} \right) \sigma$$
$$+ \frac{\lambda_\rho}{\Lambda} \left(\bar{L}_{iL}^c i\sigma_2 \Delta L_{jL} \right) \rho + \text{H.c.}, \quad (3.1)$$

where Λ is a cutoff scale, i, j are generation indices, and $\lambda_\Phi, \lambda_\sigma$, and λ_ρ are independent parameters associated with the flavon fields Φ, σ, and ρ, respectively. The S_4 breaking to one of its Z_2 subgroups is realized when the flavon fields acquire VEVs along the directions

$$\langle \Phi \rangle = v_\Phi (1, 1, 1)^T,$$
$$\langle \sigma \rangle = v_\sigma (1, 0)^T,$$
$$\langle \rho \rangle = v_\rho. \quad (3.2)$$

Using the S_4 tensor product rules given in the Appendix, we obtain the following neutrino mass matrix:

$$m_\nu = v_\Delta \begin{pmatrix} 2a+b & -a-c & -a \\ -a-c & 2a & -a+b \\ -a & -a+b & 2a-c \end{pmatrix}, \quad (3.3)$$

where a, b, c are parameters that can be expressed in terms of the flavon VEVs and λ_i,

$$a = \frac{\lambda_\Phi v_\Phi}{\Lambda}, \qquad b = \frac{\lambda_\rho v_\rho}{\Lambda}, \qquad c = \frac{\lambda_\sigma v_\sigma}{\Lambda}. \quad (3.4)$$

In order to account for CP violation in the neutrino sector, it is necessary for the parameter c to be a complex valued parameter, i.e., $c \to |c|e^{i\phi_c}$, where ϕ_c is a CP violating phase. In the case where $c = 0$, m_ν exhibits the $\mu - \tau$ symmetry [33–37] which yields to a tribimaximal mixing matrix (TBM) [38], known for its conservation of CP symmetry. Therefore, the presence of the parameter c breaks this $\mu - \tau$ symmetry giving rise to a neutrino mass matrix characterized by the magic symmetry [39]. This term alludes to the intriguing property that the sum of elements within any row or column of m_ν remains constant and that m_ν is diagonalized by the well-known trimaximal mixing matrix (U_{TM_2}) which is expressed in terms of an arbitrary angle θ and a phase η which will be related to the neutrino oscillation parameters. Since the parameter c is responsible for small deviations from the TBM texture, the modulus of c must satisfy: $|c| < a, b$. Accordingly, by diagonalizing m_ν we find the following eigenvalues valid up to corrections of order $\mathcal{O}(|c|^2)$

$$|m_1| = v_\Delta \sqrt{(3a+b)(3a+b+|c|\cos\phi_c)},$$
$$|m_2| = v_\Delta \sqrt{b^2 - 2b|c|\cos\phi_c},$$
$$|m_3| = v_\Delta \sqrt{(3a-b)(3a-b-|c|\cos\phi_c)}. \quad (3.5)$$

The diagonalization of m_ν by U_{TM_2} induces relations between the model parameters $\{a, b, |c|, \phi_c\}$ and the trimaximal mixing parameters θ and η which are found to be

$$\tan 2\theta = -\frac{|c|\sqrt{9a^2\cos^2\phi_c + b^2\sin^2\phi_c}}{\sqrt{3}a(b+|c|\cos\phi_c)},$$
$$\tan\eta = \frac{b}{3a}\tan\phi_c. \quad (3.6)$$

From Eq. (3.5), we derive the expressions for the solar and atmospheric mass-squared differences,

$$\Delta m_{21}^2 = -3v_\Delta^2(|c|\cos\phi_c(a+b) + a(3a+2b)),$$
$$\Delta m_{31}^2 = -6v_\Delta^2 a(|c|\cos\phi_c + 2b). \quad (3.7)$$

The neutrino mixing angles are expressed in the case of TM$_2$ with respect to θ and η as follows:

$$\sin^2\theta_{12} = \frac{1}{3 - 2\sin^2\theta},$$
$$\sin^2\theta_{13} = \frac{2}{3\sin^2\theta},$$
$$\sin^2\theta_{23} = \frac{1}{2} - \frac{\sqrt{3}\sin 2\theta}{2(3 - \sin^2\theta)}\cos\eta. \quad (3.8)$$
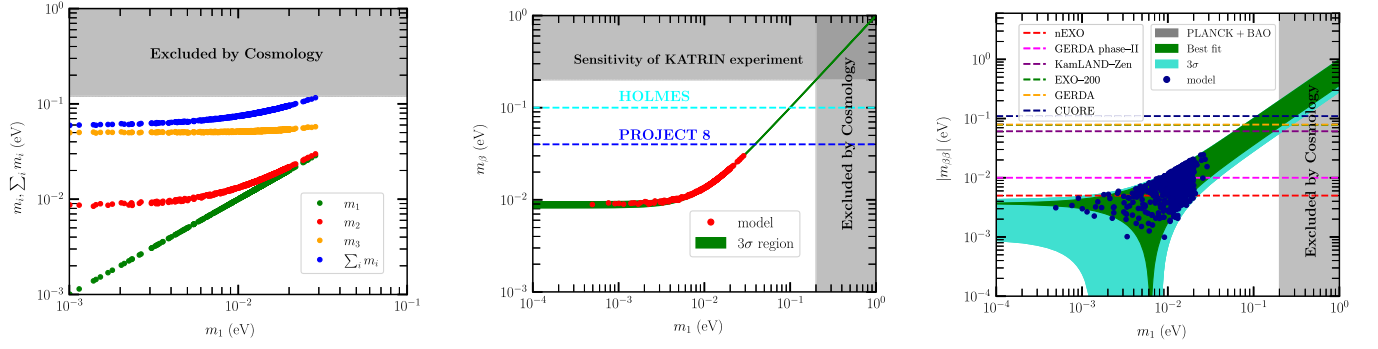
FIG. 5. Left: prediction for the absolute neutrino masses and their sum Σm_i as a function of m_1. Middle: m_β as a function of m_1 where the vertical and horizontal gray regions are disfavored by Planck and KATRIN Collaborations, respectively, while the horizontal dashed lines represent the future sensitivities on m_β from HOLMES and Project 8 Collaborations. Right: $|m_{\beta\beta}|$ as a function of m_1 where the horizontal dashed lines represent the limits on $|m_{\beta\beta}|$ from current and future $0\nu\beta\beta$ decay experiments.

Moreover, by matching the expression of the Jarlskog parameter from the PDG standard parametrization [40], and its expression derived from the trimaximal mixing matrix $J_{CP} = (1/6\sqrt{3})\sin 2\theta \sin \eta$, we can establish a relationship between η, the Dirac CP phase and the atmospheric angle that will be used as a constraint in our numerical calculations

$$\sin 2\theta_{23} \sin \delta_{CP} = \sin \eta. \qquad (3.9)$$

There are three different sources that can be used to probe the absolute values of neutrino-mass eigenvalues: (1) the sum of the three active neutrino masses from cosmological observations $\sum_i m_i = m_1 + m_2 + m_3$; (2) direct determination of the neutrino mass by measuring the energy spectrum of the electrons produced in the β-decay of nuclei which allows to get information on the effective electron antineutrino mass defined by $m_\beta = (\sum_i m_i^2 |U_{ei}|^2)^{1/2}$, where U_{ei} are the elements of the first row of the neutrino mixing matrix (the current limit from tritium beta decay is given by the KATRIN project, which aims at a detection of m_β with a sensitivity of 0.2 eV [41]); (3) the search for neutrinoless double beta decay ($0\nu\beta\beta$) processes whose decay amplitude is proportional to the effective Majorana

neutrino mass defined as $|m_{\beta\beta}| = |\sum_i U_{ei}^2 m_i|$. There are many ongoing and upcoming experiments which aim to achieve a sensitivity up to 0.01 eV for $|m_{\beta\beta}|$. In the context of the trimaximal mixing, U_{ei} in m_β and $|m_{\beta\beta}|$ are replaced by the elements of the first row of U_{TM_2} while the masses m_i are as given in Eq. (3.5). For $m_{\beta\beta}$, two additional phases are introduced and the full mixing matrix can be written as $U_{\mathrm{TM}_2} U_P$ where $U_P = \mathrm{diag}(1, e^{i\alpha_{21}/2}, e^{i\alpha_{31}/2})$ with α_{21} and α_{31} being two extra Majorana phases. Since the recent results from NuFiT Collaboration show a mild preference for the normal neutrino mass hierarchy [1], we will perform a brief numerical analysis of neutrino masses in the case where $m_1 < m_2 \lesssim m_3$. By taking into account the 3σ C.L. of the oscillation parameters from Ref. [1], and the upper bound on the sum of neutrino masses from the latest Planck data $\sum m_i < 0.12$ eV at 95% C.L. [42], we show in Fig. 5 the three neutrino masses and their sum (left panel), m_β (middle panel), and $|m_{\beta\beta}|$ (right panel) as a function of the lightest neutrino mass m_1. Here, we assume that the angle θ is allowed to vary in the range $[0, \pi/2]$, and the phases η, ϕ_c, α_{21}, and α_{31} are randomly varied in the range $[0, 2\pi]$ while the parameters a, b, and c are varied in the range $[-1, 1]$. From Fig. 5, the predicted regions for $m_{i=1,2,3}$, $\sum_i m_i$, m_β and $|m_{\beta\beta}|$ are as follows:

$$0.00049 \lesssim m_1 \ [\mathrm{eV}] \lesssim 0.02866, \qquad 0.00834 \lesssim m_2 \ [\mathrm{eV}] \lesssim 0.02986, \qquad 0.04941 \lesssim m_3 \ [\mathrm{eV}] \lesssim 0.05754,$$

$$0.05884 \lesssim \sum m_i \ [\mathrm{eV}] \lesssim 0.11607, \qquad 0.00889 \lesssim m_\beta \ [\mathrm{eV}] \lesssim 0.03001, \qquad 0.00099 \lesssim |m_{\beta\beta}| \ [\mathrm{eV}] \lesssim 0.02438. \quad (3.10)$$

The predicted upper bound value of $\sum m_i$ is close to the result of the Planck Collaboration [42], while the lower bound (~ 0.06 eV) requires further studies in future cosmological data and may be tested in the future by experiments such as CORE + BAO aiming to reach a 0.062 eV sensitivity [43]. For m_β, the obtained values are far from the

forthcoming β-decay experiment sensitivities [44–47], and thus require experiments with improved sensitivities around 0.02 eV. For $|m_{\beta\beta}|$, the horizontal dashed lines in Fig. 5 show that the model values are below the current sensitivities for some of the ongoing $0\nu\beta\beta$ decay experiments while the anticipated sensitivities of the next-generation experiments

such as GERDA Phase II [48] and nEXO [49] will cover our model predictions on $|m_{\beta\beta}|$. Moreover, it is clear from the mass expressions in Eq. (3.5) that the tiny neutrino masses constraint the parameter v_Δ, which has been determined to fall within the range of $0.01803 \lesssim v_\Delta \, [\text{eV}] \lesssim 0.04997$.

B. Solution to the DW problem

1. Exploring the DW problem and potential remedies

As outlined above, DWs are sheetlike topological defects that emerge as a result of the SSB of discrete groups. These two-dimensional structures remain stable when the vacuum manifold, defined by the scalar potential of the theory, is topologically nontrivial. This nontriviality manifests as isolated points corresponding to distinct degenerate ground states within the theory. In the classic example of SSB of the discrete Z_2 symmetry driven by a real scalar field transforming as $\varphi \to -\varphi$, the potential has two degenerate vacua at $\varphi = \pm v$. Thus, the associated manifold is restricted to only two points. In our toy model where S_4 breaks down to Z_2, the manifold is made of twelve disconnected vacua given by the quotient group S_4/Z_2 which corresponds to the broken part $V_4 \rtimes Z_3$ as discussed in Sec. II. Once the scalar field settle into one of these possible ground states representing a point within the vacuum manifold, depicted graphically as the cuboctahedron in Fig. 4, it becomes impossible to transition to another point within the manifold. The transitional regions between these degenerate ground states are what we refer to as DWs.

In order to understand why stable DWs are problematic, it is essential to comprehend the cosmological implications of the SSB of a discrete group. According to the standard cosmological model, the initial state of the Universe is a state of local thermal equilibrium at extremely high temperature. Typically, spontaneously broken symmetries are restored at this high temperature. However, as the Universe goes through cosmic expansion and gradually cools over time, a crucial phase transition takes place when the temperature falls below a critical threshold leading to the SSB of the discrete symmetry. The issue arises from the fact that distinct regions with a characteristic size of approximately the Hubble radius H^{-1} become causally disconnected. After the symmetry is broken, these regions will be situated in different vacua, separated by DWs. A comprehensive study of the cosmological evolution of a Universe containing these DWs was first performed by Zel'dovich, Kobzarev, and Okun [4], where they concluded that the contribution of stable DWs to the energy density of the Universe would rapidly surpass the contribution from radiation, causing a rapid expansion of the Universe that would leave less time for the formation of galaxies and subsequently impact the production rates during big bang nucleosynthesis. Indeed, the energy density of DWs can be expressed as

$$\rho_{\text{DW}} = \sigma_{\text{DW}}/R, \qquad (3.11)$$

where R represents the typical size of the DWs, and σ_{DW} denotes the surface energy density of the walls. The parameter R is directly proportional to the scale factor a, and thus the energy density of domain walls scales as a^{-1}, which is significantly lower than the scaling of radiation a^{-4} or matter a^{-3}. This means that as time progresses, the energy density of DWs decreases at a slower rate than that of matter or radiation. Eventually, regardless of their initial abundance, their presence at late times would make them the dominant contributors to the total energy density of the Universe. This has profound cosmological implications that conflicts observational data, notably leaving significant imprints in the CMB radiation. To elaborate this point, recall that the CMB exhibits an incredibly precise blackbody radiation [50], and any deviation from this spectrum, referred to as CMB spectral distortions, holds invaluable information about the physics of the early Universe. Specifically, the primordial fluctuations of matter density, that will later form large-scale structures we observe today, leave imprints in the form of temperature anisotropies in the CMB. Nevertheless, these temperature fluctuations are very small, with the CMB spectrum maintaining remarkable uniformity up to about 1 part in 10^5, usually expressed as

$$\frac{\delta T}{T} \lesssim 10^{-5}, \qquad (3.12)$$

where δT denotes the temperature deviation in a given region of the sky, and T denotes the mean temperature of the CMB. With these cosmic evolution facts in mind, a notable challenge that arises with the existence of stable DWs within the observable Universe is that they would introduce additional distortions, or excessive anisotropies, in contrast to the CMB anisotropies that we observe today. This issue emerges particularly in cases where the symmetry breaking scale is around $v_\varphi \gtrsim 1$ MeV as shown in Ref. [4]. This bound is estimated by equating the density fluctuation $\delta\rho_{\text{DW}}/\rho_{\text{DW}}$ of a DW to the temperature fluctuation in the CMB, $\delta T/T$, which are approximately equal at the surface of the last scattering (postrecombination) when the DW spans across the present observable horizon [6]. The density fluctuation for a DW located between two degenerate vacua is estimated to be

$$\frac{\delta\rho_{\text{DW}}}{\rho_{\text{DW}}} \sim 10^{60} \times \left(\frac{v_\varphi}{M_{\text{Planck}}}\right)^3, \qquad (3.13)$$

where $M_{\text{Planck}} = 1.2 \times 10^{19}$ GeV is the Planck mass. Consequently, the constraint $\delta\rho_{\text{DW}}/\rho_{\text{DW}} \sim \delta T/T \lesssim 10^{-5}$ establishes a lower limit on v_φ; $v_\varphi \gtrsim 1$ MeV under which stable DWs pose significant cosmological challenges. Conversely, these DWs do not present any issues if the gravitational redshift of the walls remain well below the

detectable threshold for anisotropy constraints, $\delta T/T \lesssim 10^{-5}$. This implies that the energy scale of the phase transition that generates these DWs must be limited to values smaller than 1 MeV.

Considering the strict constraint imposed on the scale of the SSB mentioned above, different approaches have been proposed in the literature to address the DW issue. These approaches revolve around the concept of unstable DWs that experience early decay, implying their existence for only a brief period of time [7]. The most famous approach is inflation [51], which is a valid solution provided that the DWs formed prior to the end of inflation, causing them to expand beyond our current observable horizon. In simpler terms, this implies that the discrete symmetry must have already broken before the onset of inflation (the phase transition must occur before the inflation). Consequently, inflation will cause these DWs to expand and disappear from our observable Universe, eliminating the associated problem. A second approach for addressing the DW problem assumes that the discrete symmetry connecting the vacuum states as approximate symmetry. This suggests the existence of an explicit symmetry breaking term, which would result in the eventual collapse of the DWs during early cosmic times [6]. It was shown in Refs. [4,5] that this can be achieved by introducing a biased potential that can effectively lift the degeneracy among the vacua. This allows one of the vacuum states to attain a slightly lower energy density than the others, ultimately establishing its dominance in the Universe as the true vacuum. Typically, this symmetry breaking term is introduced by hand, although in principle, the soundness of this solution depends on whether explicit breaking naturally arises from some underlying physics [52]. Indeed, it was shown in Refs. [12,53] that this explicit breaking term can be achieved by taking into account Planck scale gravitational effects. This is realized via the introduction of higher-dimensional operators, denoted as

$$\frac{1}{M_{\text{Planck}}^n} O_{n+4} + \text{H.c.}, \tag{3.14}$$

which are suppressed by powers of the Planck mass M_{Planck} in the scalar potential leading to a preference for one of the vacua over the others. In fact, it is widely believed that all global symmetries are expected to be explicitly broken by quantum gravitational effects, and yet may play an important role in particle physics and cosmology. These general expectations are supported by theoretical calculations illustrating the explicit breaking of global symmetries by sources such as black holes [54]. In addition, it has been shown that certain concrete theories of quantum gravity do not admit exact global symmetries, including holography [55] and string theory [56]. The same concept is applicable to our S_4 toy model, which features twelve degenerate vacua. By introducing a slight bias in favor of one vacuum state over the others, we effectively resolve the DW problem.

2. Solving the DW problem within our toy model

In the toy model outlined above, the S_4 flavor symmetry is broken into one of the Z_2 subgroups of S_4 with the broken part denoted as $K_4 \rtimes Z_3 \subset S_4$. This breaking is realized by one of the flavons listed in Table I. As a result, DWs form, and expand between the boundaries of twelve degenerate vacua $\phi_{i=1,\dots,12}$ which are distinguished by the transformation of the broken part $K_4 \rtimes Z_3$ as detailed in Sec. II C 4. These DWs pose a challenge when the scale of the symmetry breaking associated with their formation falls below the inflationary scale which is approximately 10^{16} GeV [57–59]. In our toy model, there is no inherent constraint preventing the VEVs of the flavons $\{\Phi, \sigma, \rho\}$ to fall below the inflationary scale threshold. Let us verify this by getting an estimate on the S_4 breaking scale using, as an example, the expression of $|m_2|$ given in Eq. (3.5). The upper bound of this mass, $|m_2| \approx 0.0298$ eV, is given in Eq. (3.10) and is obtained for

$$v_\Delta \approx 0.047 \text{ eV}, \qquad b \approx 0.827,$$
$$|c| \approx 0.198, \qquad \cos\phi_c = 0.875. \tag{3.15}$$

From the expressions of $|c| = \frac{\lambda_\sigma v_\sigma}{\Lambda}$ and $b = \frac{\lambda_\rho v_\rho}{\Lambda}$, and assuming for simplicity that the Yukawa couplings are of order $\mathcal{O}(1)$, it is clear that when considering the VEV of flavons ρ and σ around the TeV scale, Λ will always remain below the inflationary scale. Therefore, we assert that the DWs created during S_4 symmetry breaking are inconsistent with the standard cosmology [60], and must be prevented.

For this purpose, we adopt the second approach mentioned above and we break explicitly the $K_4 \rtimes Z_3$ subgroup of S_4 at a high energy scale by using one of the possible Planck-suppressed operators within our toy model. The leading higher-dimensional terms induced by gravity and respecting gauge invariance are of dimension five, thus they are suppressed by one power of M_{Planck}. It is worth noting that due to the substantial suppression of these operators, the model remains unchanged at lower energy scales.

There exist several five-dimensional operators capable of explicitly breaking the S_4 flavor group. However, it is not necessary to enumerate or employ all of them. As stated in Ref. [60], even the tiny higher-dimensional symmetry-breaking terms, constrained by powers of the Planck mass, may suffice to address the DW problem. Given our primary focus on S_4 flavon triplets, we shall employ the flavon triplet $\Phi \sim \mathbf{3}$. During the SSB of the S_4 group, this triplet creates DWs that are located on the boundaries of the twelve degenerate vacua as described in Eq. (2.22) and depicted in Fig. 4. Therefore, the leading contribution of Φ in the effective scalar potential may be expressed as

$$\Delta V_{\text{eff}} = \frac{\varepsilon_5}{M_{\text{Planck}}}[[(\Phi^\dagger\Phi)_\mathbf{3}(\Phi^\dagger\Phi)_\mathbf{3}]_{\mathbf{3}'}(\Phi^\dagger)_\mathbf{3}]_{\mathbf{1}'} + \text{H.c.}], \quad (3.16)$$

where ε_5 is a positive dimensionless parameter that characterizes the effective bias. Since this term transforms as a nontrivial S_4 singlet it breaks explicitly the S_4 group. When the flavon triplet obtains its VEV, $\langle\Phi\rangle = (v_\Phi, v_\Phi, v_\Phi)^T$, the resulting contribution from ΔV_{eff} becomes sufficient to lift the degeneracy among the twelve degenerate vacua $\phi_{i=1,\dots,12}$. In such a scenario, the energy-density difference between these vacua can be approximated as

$$V_{\text{bias}} \approx \frac{\varepsilon_5 v_\Phi^5}{M_{\text{Planck}}}, \quad (3.17)$$

where v_Φ represents the scale of spontaneous symmetry breaking of the S_4 group. Therefore, to estimate the amount of symmetry breaking, it is necessary to determine the values of the bias coefficient ε_5. Assuming that this coefficient is real, the general condition for the elimination of DWs, taking into account the operator mentioned in Eq. (3.16) can be expressed as follows [60]:

$$\varepsilon_5 > \left(\frac{v_\Phi}{M_{\text{Planck}}}\right). \quad (3.18)$$

As previously discussed, there is no inherent constraint preventing SSB of S_4 from occurring at scales lower than that of inflation. In fact, as the scale of symmetry breaking decreases, the possibility of creating an energy gap among the degenerate vacua becomes increasingly plausible [61]. The minimum size of symmetry breaking depends on both ε_5 and v_Φ. For instance, if we consider v_Φ to be around the TeV scale, it is sufficient to require that $\varepsilon_5 > 10^{-17}$ in order to favor one of the vacuum states over the others. Moreover, by using Eq. (III.39) and assuming that $v_\Phi \approx \mathcal{O}(1)$ TeV, a quantitative estimate of the minimum symmetry breaking size required to solve the DW problem can be written as

$$V_{\text{bias}} > 10^{-17} \ (\text{GeV})^3 \frac{v_\Phi^2}{M_{\text{Planck}}} \approx 10^{-21} \ (\text{GeV})^4.$$

Therefore, the nonrenormalizable operator given in Eq. (3.15) gives rise to an extremely small contribution in the low-energy regime and hence will have negligible effect on e.g., the neutrino sector.

3. Gravitational waves from DWs

The dimension-five operator in Eq. (3.16) induces a slight bias among degenerate minima, ultimately favoring one true vacuum state. Over time, this bias becomes dynamically significant, accelerating each wall towards its adjacent higher-energy vacuum and driving the evolution of the DWs towards their eventual annihilation. The dynamics of these walls can be fully understood if two underlying forces

are determined. The first one is the surface tension (p_T) caused by the curvature and is proportional to the energy per unit area; $p_T \sim \sigma_{\text{DW}}/R$. This force acts as a surface pressure that straightens the curved walls up to the horizon scale. The second force is the volume pressure which shrinks the false vacuum domains leading to the collapse of DWs and is approximately scaling as $p_V \sim vT^4$ [62], where v is the velocity of the DWs. This force is equal to the differences in energy density of the vacua and thus may be expressed also as $p_V \sim V_{\text{bias}} = (\varepsilon_5 v_\Phi^5)/M_{\text{Planck}}$. These two forces compete, and the dynamics of the walls is profoundly influenced by the magnitude of the bias [7]. DWs annihilate when the pressure p_V becomes comparable to the tension force p_T. This annihilation process is remarkably energetic, resulting in the emission of stochastic GWs which retain various information on the physics of the early Universe [61,63–67]. The time of annihilation t_{ann} and the corresponding temperature T_{ann} are given by

$$t_{\text{ann}} \simeq \frac{\sigma_{\text{DW}}}{V_{\text{bias}}},$$

$$T_{\text{ann}} = 3 \times 10^7 \left(\frac{10}{g_*(T_{\text{ann}})}\right)^{1/4} \left(\frac{V_{\text{bias}}\sigma_{\text{DW}}^{-1}}{1 \ \text{TeV}}\right)^{1/2} \text{TeV}, \quad (3.19)$$

where $g_*(T_{\text{ann}})$ is the effective number of degrees of freedom at t_{ann}. In most realistic cases, $(10/g_*)^{1/4}$ is of order one. Using the expression of V_{bias} in Eq. (3.17), we have

$$t_{\text{ann}} \simeq \frac{\sigma_{\text{DW}} M_{\text{Planck}}}{\varepsilon_5 v_\Phi^5},$$

$$T_{\text{ann}} \simeq 3 \times 10^7 \left(\frac{\varepsilon_5 v_\Phi^5 \sigma_{\text{DW}}^{-1} M_{\text{Planck}}^{-1}}{1 \ \text{TeV}}\right)^{1/2} \text{TeV}. \quad (3.20)$$

Once the tension force becomes dominant, DWs will enter the scaling regime in which the typical length scales are given by the Hubble radius H^{-1} as mentioned previously. This is the so-called scaling solution, for which the energy density of the DWs evolves as $\rho_{\text{DW}} = \mathcal{A}\sigma_{\text{DW}}/t$ where $\mathcal{A}$ is a dimensionless numerical factor called the area parameter which takes an almost constant value [67].[6] In this scaling regime, the peak amplitude of the stochastic GWs spectrum at the present time t_0 can be expressed as [67,71]

---

[6]The scaling properties of DWs have been verified through several numerical [67] and analytical [68] techniques. For instance, using numerical simulations in a model with two degenerate vacua (Z_2-invariant scalar potential), it has been found that the parameter $\mathcal{A}$ approximates to $\mathcal{A} \simeq 0.8 \pm 0.1$. In models with $N > 2$ degenerate vacua, this parameter is usually estimated based on the Z_2 example and its value increases proportionally with N [69,70]. In Ref. [71], the value of $\mathcal{A}$ was estimated as $\mathcal{A} \simeq 0.8 \times (3/2)$ in a model with three degenerate vacua (i.e., Z_3 invariant NMSSM).

$$\Omega_{\mathrm{GW}}h^2(t_0)|_{\mathrm{peak}} \simeq 5.2 \times 10^{-20} \tilde{\epsilon}_{\mathrm{gw}} \mathcal{A}^4 \left(\frac{10.75}{g_*(T_{\mathrm{ann}})}\right)^{1/3}$$

$$\times \left(\frac{\sigma_{\mathrm{DW}}}{1~\mathrm{TeV}^3}\right)^4 \left(\frac{1~\mathrm{MeV}^4}{V_{\mathrm{bias}}}\right)^2, \qquad (3.21)$$

where $\tilde{\epsilon}_{\mathrm{gw}}$ is an efficiency parameter determined in numerical simulations to be equal to $\tilde{\epsilon}_{\mathrm{gw}} \simeq 0.7$ [67]. Beyond the peak, the amplitude of GWs spectrum induced by collapsing DWs is given by

$$\Omega_{\mathrm{GW}}h^2 \simeq \Omega_{\mathrm{GW}}h^2|_{\mathrm{peak}} \times \begin{cases} \left(\frac{f}{f_{\mathrm{peak}}}\right)^3, & f < f_{\mathrm{peak}} \\ \frac{f}{f_{\mathrm{peak}}}, & f > f_{\mathrm{peak}}, \end{cases} \qquad (3.22)$$

where the peak frequency is found to be

$$f(t_0)_{\mathrm{peak}} \simeq 3.99 \times 10^{-19} \times \mathcal{A}^{-1/2} \times \left(\frac{1~\mathrm{TeV}^3}{\sigma_{\mathrm{DW}}}\right)^{1/2}$$

$$\times \left(\frac{V_{\mathrm{bias}}}{1~\mathrm{MeV}^4}\right)^{1/2}~\mathrm{Hz}. \qquad (3.23)$$

It is clear from Eqs. (3.21) and (3.23) that both the amplitude and the peak frequency of the GWs depend on two parameters; σ_{DW} and V_{bias}. Since both σ_{DW} and V_{bias} depend on the scale of the SSB of S_4 symmetry (v_Φ), the spectrum of $\Omega_{\mathrm{GW}}h^2$ can be used to constrain the SSB of S_4 within this model. It is worth noting that the same scale (v_Φ) controls some of the neutrino predictions. Therefore, detailed analyses will shed some lights on the connections between flavor symmetries, neutrino mass and the DW problem through GWs.

Our primary goal in this paper is to discuss the theoretical and geometric aspects of the DW problem arising from the spontaneous breaking of the S_4 flavor symmetry into its potential residual symmetries. While we have outlined the subtleties of GWs using parameters from our toy model, more involved analyzes of GW probes of DWs within models based on non-Abelian discrete groups necessitate further investigations of the wall network that relies in part on dedicated Monte Carlo simulations which we leave for a future work.

IV. SUMMARY AND CONCLUSIONS

In this work, we have studied the formation of cosmic DWs from the SSB of the S_4 discrete group. This breaking occurs when gauge singlet flavon fields acquire VEVs giving rise to multiple distinct degenerate vacua separated by energy barriers which establish a network of DWs. These non-Abelian discrete groups are widely used in flavor model building, primarily because of their ability to give predictions that are in good agreement with neutrino oscillation data. In these models, a crucial point is that there are distinct preserved residual symmetries in the neutrino and charged lepton sectors after the SSB. This distinction arises from the fact that the flavon configurations that predict specific fermion mass structures exhibit different VEV directions in both sectors. Consequently, the number of vacua is contingent upon both the order of the residual symmetry and the order of the underlying flavor group. In the case of the S_4 flavor symmetry, we have investigated three possible breaking patterns that are phenomenologically viable: $S_4 \to K_4$, $S_4 \to Z_3$, and $S_4 \to Z_2$. The associated broken subgroups are given by the non-Abelian groups $S_3 \simeq S_4/K_4$, $\Sigma(8) \simeq S_4/Z_3$, and $A_4 \simeq S_4/Z_2$, respectively. Therefore, the number of vacua for each breaking pattern is given by the order of S_3, $\Sigma(8)$, and A_4, namely 6, 8, and 12 respectively. The challenges associated with presenting DWs in cases of multiple vacua have been addressed through a novel approach where we have depicted the S_4 DW networks by representing each breaking pattern's multiple vacua as vertices. Each vertex is expressed through vector coordinates in flavon space. The resulting outcome consists of Archimedean or Platonic solids, created by connecting vertices that represent degenerate vacua with edges that symbolize DWs. This provides a clear visualization of the intricate network structure.

On the other hand, we addressed the challenge of stable DWs by introducing an S_4 toy model wherein neutrino masses are generated through the type-II seesaw mechanism. After the SSB of gauge and flavor symmetries, the resulting neutrino mass matrix exhibits a magic symmetry, and it is diagonalized by the trimaximal mixing matrix known to align with neutrino oscillation data. Moreover, we find that the obtained predictions concerning the sum of the three active neutrino masses $\sum m_i$, and the effective Majorana mass $m_{\beta\beta}$ can be probed by future experiments. The breaking pattern in this toy model is given by $S_4 \to Z_2$, which gives rise to twelve degenerate vacua, and to resolve the DW problem, we have adopted the approach of explicit symmetry breaking through the introduction of a Planck-suppressed operator induced by gravity into the scalar potential. This explicit breaking induces a bias among the twelve degenerate vacua, parameterized as $\varepsilon_5 v_\Phi^5$, where v_Φ is the scale of the SSB of the S_4 group. Lifting the degeneracy of the multiple minima of the scalar potential while favoring one true vacuum state is obtained by putting constraints on the dimensionless coefficient ε_5 that characterized the bias where we find that for $v_\Phi \sim \mathcal{O}(1)$ TeV, it is sufficient to require $\varepsilon_5 > 10^{-17}$ in order to drive the evolution of the walls towards their annihilation.

An interesting outcome of the annihilation of DWs is the production of GWs, offering a potential avenue for probing these models through ongoing and planned GW experiments. However, accurately describing gravitational wave emission in models based on non-Abelian discrete groups necessitates a thorough examination of the parameters influencing the evolution of the formed walls. This involves undertaking dedicated numerical simulations, presenting a

complex scenario in contrast to the well-established examples found in literature with Z_2 symmetry. A thorough examination of this topic is reserved for future investigations.

APPENDIX: THE S_4 GROUP

The flavor group S_4 is the permutation group of four distinct objects. It contains 24 elements which can be generated by three generators $\mathcal{T}$, $\mathcal{S}$, and $\mathcal{U}$ satisfying $\mathcal{S}^2 = \mathcal{T}^3 = \mathcal{U}^2 = (\mathcal{ST})^3 = (\mathcal{SU})^2 = (\mathcal{TU})^2 = (\mathcal{STU})^4 = I$. Through the standard relation connecting the number of elements with the dimension of the irreducible representations of S_4—$24 = 1^2 + 1^2 + 2^2 + 3^2 + 3^2$—we deduce that S_4 contains five real irreducible representations where we have two singlets **1** (trivial) and **1′**, one doublet **2**, and two triplets **3** and **3′**. The character table of S_4 is shown in

TABLE II. Characters of the irreducible representations of the S_4 group.

Classes	χ_1	$\chi_{1'}$	χ_2	χ_3	$\chi_{3'}$
$\mathcal{C}_1$	1	1	2	3	3
$\mathcal{C}_3$	1	1	2	−1	−1
$\mathcal{C}_6$	1	−1	0	−1	1
$\mathcal{C}_8$	1	1	−1	0	0
$\mathcal{C}_6'$	1	−1	0	1	−1

Table II where the index in $\mathcal{C}_i$ indicates the number of elements in each conjugacy class which are given explicitly as follows:

$$\mathcal{C}_1 = \{1\}, \qquad \mathcal{C}_3 = \{\mathcal{S}, \mathcal{TST}^2, \mathcal{T}^2\mathcal{ST}\},$$
$$\mathcal{C}_6 = \{\mathcal{U}, \mathcal{TU}, \mathcal{SU}, \mathcal{T}^2\mathcal{U}, \mathcal{STSU}, \mathcal{ST}^2\mathcal{SU}\},$$
$$\mathcal{C}_8 = \{\mathcal{T}, \mathcal{ST}, \mathcal{TS}, \mathcal{STS}, \mathcal{T}^2, \mathcal{ST}^2, \mathcal{T}^2\mathcal{S}, \mathcal{ST}^2\mathcal{S}\},$$
$$\mathcal{C}_6' = \{\mathcal{STU}, \mathcal{TSU}, \mathcal{T}^2\mathcal{SU}, \mathcal{ST}^2\mathcal{U}, \mathcal{TST}^2\mathcal{U}, \mathcal{T}^2\mathcal{STU}\}. \quad \text{(A1)}$$

The representation matrices for the S_4 generators $\mathcal{T}$, $\mathcal{S}$, and $\mathcal{U}$ in the basis where $\mathcal{T}$ is diagonal are of the following form for the five different representations:

$$\mathbf{1}_{(1,1,1)}: \quad \mathcal{S} = 1 \quad \mathcal{T} = 1 \quad \mathcal{U} = 1,$$

$$\mathbf{1}'_{(1,1,-1)}: \quad \mathcal{S} = 1 \quad \mathcal{T} = 1 \quad \mathcal{U} = -1,$$

$$\mathbf{2}_{(2,-1,0)}: \quad \mathcal{S} = \begin{pmatrix} 1 & 0 \\ 0 & 1 \end{pmatrix} \quad \mathcal{T} = \begin{pmatrix} \omega & 0 \\ 0 & \omega^2 \end{pmatrix} \quad \mathcal{U} = \begin{pmatrix} 0 & 1 \\ 1 & 0 \end{pmatrix},$$

$$\mathbf{3}_{(-1,0,-1)}: \quad \mathcal{S} = \frac{1}{3}\begin{pmatrix} -1 & 2 & 2 \\ 2 & -1 & 2 \\ 2 & 2 & -1 \end{pmatrix} \quad \mathcal{T} = \begin{pmatrix} 1 & 0 & 0 \\ 0 & \omega^2 & 0 \\ 0 & 0 & \omega \end{pmatrix} \quad \mathcal{U} = -\begin{pmatrix} 1 & 0 & 0 \\ 0 & 0 & 1 \\ 0 & 1 & 0 \end{pmatrix},$$

$$\mathbf{3}'_{(-1,0,1)}: \quad \mathcal{S} = \frac{1}{3}\begin{pmatrix} -1 & 2 & 2 \\ 2 & -1 & 2 \\ 2 & 2 & -1 \end{pmatrix} \quad \mathcal{T} = \begin{pmatrix} 1 & 0 & 0 \\ 0 & \omega^2 & 0 \\ 0 & 0 & \omega \end{pmatrix} \quad \mathcal{U} = \begin{pmatrix} 1 & 0 & 0 \\ 0 & 0 & 1 \\ 0 & 1 & 0 \end{pmatrix}, \quad \text{(A2)}$$

where ω is the cube root of unity: $\omega = e^{2\pi i/3}$. There are 30 subgroups of S_4, twenty of which are Abelian groups. These are nine Z_2, four Z_3, three Z_4, and four Klein four group $K_4 \simeq Z_2 \times Z_2$ generated by

$$Z_2: \ \mathcal{S}, \mathcal{TST}^2, \mathcal{T}^2\mathcal{ST}, \mathcal{U}, \mathcal{SU}, \mathcal{TU}, \mathcal{T}^2\mathcal{U}, \mathcal{STSU}, \mathcal{ST}^2\mathcal{SU},$$
$$Z_3: \mathcal{T}, \mathcal{ST}, \mathcal{TS}, \mathcal{STS},$$
$$Z_4: \mathcal{ST}^2\mathcal{U}, \mathcal{TSU}, \mathcal{TST}^2\mathcal{U},$$
$$K_4: \{\mathcal{S}, \mathcal{TST}^2\}, \{\mathcal{S}, \mathcal{U}\}, \{\mathcal{TST}^2, \mathcal{T}^2\mathcal{U}\}, \{\mathcal{T}^2\mathcal{ST}, \mathcal{TU}\}. \quad \text{(A3)}$$

Let us now provide the Kronecker products among the irreducible representations of the S_4 group. The products between two representations are presented as follows:

$$\mathbf{1} \otimes \mathbf{R} = \mathbf{R}, \qquad \mathbf{1'} \otimes \mathbf{1'} = \mathbf{1}, \qquad \mathbf{1'} \otimes \mathbf{2} = \mathbf{2}, \qquad \mathbf{1'} \otimes \mathbf{3} = \mathbf{3'}, \qquad \mathbf{1'} \otimes \mathbf{3'} = \mathbf{3},$$

$$\mathbf{2} \otimes \mathbf{2} = \mathbf{1} \oplus \mathbf{1'} \oplus \mathbf{2}, \qquad \mathbf{2} \otimes \mathbf{3} = \mathbf{2} \otimes \mathbf{3'} = \mathbf{3} \oplus \mathbf{3'},$$

$$\mathbf{3} \otimes \mathbf{3} = \mathbf{3'} \otimes \mathbf{3'} = \mathbf{1} \oplus \mathbf{2} \oplus \mathbf{3} \oplus \mathbf{3'}, \qquad \mathbf{3} \otimes \mathbf{3'} = \mathbf{1'} \oplus \mathbf{2} \oplus \mathbf{3} \oplus \mathbf{3'}, \tag{A4}$$

where $\mathbf{R}$ stands for any irreducible representation of S_4. In the following we list the Clebsch-Gordan coefficients using the notations $\alpha \sim \mathbf{1}$, $\alpha' \sim \mathbf{1'}$, $(\beta_1, \beta_2)^T, (\gamma_1, \gamma_2)^T \sim \mathbf{2}$, $(a_1, a_2, a_3)^T, (b_1, b_2, b_3)^T \sim \mathbf{3}$, $(c_1, c_2, c_3)^T, (d_1, d_2, d_3)^T \sim \mathbf{3'}$. For a singlet multiplied with a doublet or a triplet we have

$$\mathbf{1} \otimes \mathbf{2} = (\alpha\beta_1, \alpha\beta_2)^T, \qquad \mathbf{1'} \otimes \mathbf{2} = (\alpha'\beta_1, -\alpha'\beta_2)^T, \qquad \mathbf{1} \otimes \mathbf{3} = (\alpha a_1, \alpha a_2, \alpha a_3)^T,$$

$$\mathbf{1'} \otimes \mathbf{3} = (\alpha'a_1, \alpha'a_2, \alpha'a_3)^T, \qquad \mathbf{1} \otimes \mathbf{3'} = (\alpha c_1, \alpha c_2, \alpha c_3)^T, \qquad \mathbf{1'} \otimes \mathbf{3'} = (\alpha'c_1, \alpha'c_2, \alpha'c_3)^T. \tag{A5}$$

For a doublet coupled to a doublet we have

$$\mathbf{2} \otimes \mathbf{2} = \begin{pmatrix} \beta_1 \\ \beta_2 \end{pmatrix} \otimes \begin{pmatrix} \gamma_1 \\ \gamma_2 \end{pmatrix} = (\beta_1\gamma_2 + \beta_2\gamma_1)_{\mathbf{1}} + (\beta_1\gamma_2 - \beta_2\gamma_1)_{\mathbf{1'}} + \begin{pmatrix} \beta_2\gamma_2 \\ \beta_1\gamma_1 \end{pmatrix}_{\mathbf{2}} \tag{A6}$$

and for a doublet multiplied with a triplet

$$\mathbf{2} \otimes \mathbf{3} = \begin{pmatrix} \beta_1 \\ \beta_2 \end{pmatrix} \otimes \begin{pmatrix} a_1 \\ a_2 \\ a_3 \end{pmatrix} = \begin{pmatrix} \beta_1 a_2 + \beta_2 a_3 \\ \beta_1 a_3 + \beta_2 a_1 \\ \beta_1 a_1 + \beta_2 a_2 \end{pmatrix}_{\mathbf{3}} + \begin{pmatrix} \beta_1 a_2 - \beta_2 a_3 \\ \beta_1 a_3 - \beta_2 a_1 \\ \beta_1 a_1 - \beta_2 a_2 \end{pmatrix}_{\mathbf{3'}},$$

$$\mathbf{2} \otimes \mathbf{3'} = \begin{pmatrix} \beta_1 \\ \beta_2 \end{pmatrix} \otimes \begin{pmatrix} c_1 \\ c_2 \\ c_3 \end{pmatrix} = \begin{pmatrix} \beta_1 c_2 - \beta_2 c_3 \\ \beta_1 c_3 - \beta_2 c_1 \\ \beta_1 c_1 - \beta_2 c_2 \end{pmatrix}_{\mathbf{3}} + \begin{pmatrix} \beta_1 c_2 + \beta_2 c_3 \\ \beta_1 c_3 + \beta_2 c_1 \\ \beta_1 c_1 + \beta_2 c_2 \end{pmatrix}_{\mathbf{3'}}. \tag{A7}$$

For the products $\mathbf{3} \otimes \mathbf{3}$ and $\mathbf{3'} \otimes \mathbf{3'}$ (with a_i, b_i to be replaced by c_i, d_i) we get

$$\mathbf{3} \otimes \mathbf{3} = \begin{pmatrix} a_1 \\ a_2 \\ a_3 \end{pmatrix} \otimes \begin{pmatrix} b_1 \\ b_2 \\ b_3 \end{pmatrix} = (a_1 b_1 + a_2 b_3 + a_3 b_2)_{\mathbf{1}} + \begin{pmatrix} a_1 b_3 + a_2 b_2 + a_3 b_1 \\ a_1 b_2 + a_2 b_1 + a_3 b_3 \end{pmatrix}_{\mathbf{2}}$$

$$+ \begin{pmatrix} a_2 b_3 - a_3 b_2 \\ a_1 b_2 - a_2 b_1 \\ a_3 b_1 - a_1 b_3 \end{pmatrix}_{\mathbf{3}} + \begin{pmatrix} 2a_1 b_1 - a_2 b_3 - a_3 b_2 \\ 2a_3 b_3 - a_1 b_2 - a_2 b_1 \\ 2a_2 b_2 - a_1 b_3 - a_3 b_1 \end{pmatrix}_{\mathbf{3'}}, \tag{A8}$$

while the Clebsch-Gordan coefficients for the product $\mathbf{3} \otimes \mathbf{3'}$ read

$$\mathbf{3} \otimes \mathbf{3'} = \begin{pmatrix} a_1 \\ a_2 \\ a_3 \end{pmatrix} \otimes \begin{pmatrix} c_1 \\ c_2 \\ c_3 \end{pmatrix} = (a_1 c_1 + a_2 c_3 + a_3 c_2)_{\mathbf{1'}} + \begin{pmatrix} a_1 c_3 + a_2 c_2 + a_3 c_1 \\ -a_1 c_2 - a_2 c_1 - a_3 c_3 \end{pmatrix}_{\mathbf{2}}$$

$$+ \begin{pmatrix} 2a_1 c_1 - a_2 c_3 - a_3 c_2 \\ 2a_3 c_3 - a_1 c_2 - a_2 c_1 \\ 2a_2 c_2 - a_1 c_3 - a_3 c_1 \end{pmatrix}_{\mathbf{3}} + \begin{pmatrix} a_2 c_3 - a_3 c_2 \\ a_1 c_2 - a_2 c_1 \\ a_3 c_1 - a_1 c_3 \end{pmatrix}_{\mathbf{3'}}. \tag{A9}$$

[1] I. Esteban, M. C. Gonzalez-Garcia, M. Maltoni, T. Schwetz, and A. Zhou, The fate of hints: Updated global analysis of three-flavor neutrino oscillations, J. High Energy Phys. 09 (2020) 178.

[2] P. F. de Salas, D. V. Forero, S. Gariazzo, P. Martínez-Miravé, O. Mena, C. A. Ternes, M. Tórtola, and J. W. F. Valle, 2020 global reassessment of the neutrino oscillation picture, J. High Energy Phys. 02 (2021) 071.

[3] F. Capozzi, E. Di Valentino, E. Lisi, A. Marrone, A. Melchiorri, and A. Palazzo, Unfinished fabric of the three neutrino paradigm, Phys. Rev. D **104**, 083031 (2021).

[4] Y. B. Zeldovich, I. Y. Kobzarev, and L. B. Okun, Cosmological consequences of the spontaneous breakdown of discrete symmetry, Zh. Eksp. Teor. Fiz. **67**, 3 (1974).

[5] T. W. B. Kibble, Topology of cosmic domains and strings, J. Phys. A **9**, 1387 (1976).

[6] A. Vilenkin, Cosmic strings and domain walls, Phys. Rep. **121**, 263 (1985).

[7] G. B. Gelmini, M. Gleiser, and E. W. Kolb, Cosmology of biased discrete symmetry breaking, Phys. Rev. D **39**, 1558 (1989).

[8] K. Nakayama, F. Takahashi, and N. Yokozaki, Gravitational waves from domain walls and their implications, Phys. Lett. B **770**, 500 (2017).

[9] W. H. Press, B. S. Ryden, and D. N. Spergel, Dynamical evolution of domain walls in an expanding universe, Astrophys. J. **347**, 590 (1989).

[10] J. C. R. E. Oliveira, C. J. A. P. Martins, and P. P. Avelino, The cosmological evolution of domain wall networks, Phys. Rev. D **71**, 083509 (2005).

[11] S. E. Larsson, S. Sarkar, and P. L. White, Evading the cosmological domain wall problem, Phys. Rev. D **55**, 5129 (1997).

[12] B. Rai and G. Senjanovic, Gravity and domain wall problem, Phys. Rev. D **49**, 2729 (1994).

[13] P. Sikivie, Of axions, domain walls and the early universe, Phys. Rev. Lett. **48**, 1156 (1982).

[14] F. Riva, Low-scale leptogenesis and the domain wall problem in models with discrete flavor symmetries, Phys. Lett. B **690**, 443 (2010).

[15] S. Chigusa, S. Kasuya, and K. Nakayama, Flavon stabilization in models with discrete flavor symmetry, Phys. Lett. B **788**, 494 (2019).

[16] S. Chigusa, S. Kasuya, and K. Nakayama, Novel flavon stabilization with trimaximal neutrino mixing, Phys. Rev. D **100**, 015030 (2019).

[17] S. Antusch and D. Nolde, Matter inflation with A_4 flavour symmetry breaking, J. Cosmol. Astropart. Phys. 10 (2013) 028.

[18] S. Chigusa and K. Nakayama, Anomalous discrete flavor symmetry and domain wall problem, Phys. Lett. B **788**, 249 (2019).

[19] S. F. King and Y.-L. Zhou, Spontaneous breaking of $SO(3)$ to finite family symmetries with supersymmetry—an A_4 model, J. High Energy Phys. 11 (2018) 173.

[20] M. A. Ouahid, M. A. Loualidi, R. A. Laamara, and E. H. Saidi, Neutrino phenomenology in the flavored NMSSM without domain wall problems, Phys. Rev. D **102**, 115023 (2020).

[21] G. B. Gelmini, S. Pascoli, E. Vitagliano, and Y.-L. Zhou, Gravitational wave signatures from discrete flavor symmetries, J. Cosmol. Astropart. Phys. 02 (2021) 032.

[22] J. Preskill, S. P. Trivedi, F. Wilczek, and M. B. Wise, Cosmology and broken discrete symmetry, Nucl. Phys. **B363**, 207 (1991).

[23] F. Bazzocchi, L. Merlo, and S. Morisi, Fermion masses and mixings in a S(4)-based model, Nucl. Phys. **B816**, 204 (2009).

[24] G. Altarelli and F. Feruglio, Tri-bimaximal neutrino mixing, A(4) and the modular symmetry, Nucl. Phys. **B741**, 215 (2006).

[25] J. S. Lomont, *Applications of Finite Groups* (Academic Press, New York, 1959).

[26] I. Girardi, S. T. Petcov, A. J. Stuart, and A. V. Titov, Leptonic Dirac CP violation predictions from residual discrete symmetries, Nucl. Phys. **B902**, 1 (2016).

[27] S. F. King and C. Luhn, Neutrino mass and mixing with discrete symmetry, Rep. Prog. Phys. **76**, 056201 (2013).

[28] S. T. Petcov and A. V. Titov, Assessing the viability of A_4, S_4 and A_5 flavour symmetries for description of neutrino mixing, Phys. Rev. D **97**, 115045 (2018).

[29] G.-J. Ding, S. F. King, and C.-C. Li, Lepton mixing predictions from S_4 in the tridirect CP approach to two right-handed neutrino models, Phys. Rev. D **99**, 075035 (2019).

[30] H. Ishimori, T. Kobayashi, H. Ohki, Y. Shimizu, H. Okada, and M. Tanimoto, Non-Abelian discrete symmetries in particle physics, Prog. Theor. Phys. Suppl. **183**, 1 (2010).

[31] X.-G. He, Y.-Y. Keum, and R. R. Volkas, A(4) flavor symmetry breaking scheme for understanding quark and neutrino mixing angles, J. High Energy Phys. 04 (2006) 039.

[32] R. Ahl Laamara, M. A. Loualidi, and E. H. Saidi, Type II seesaw supersymmetric neutrino model for $\theta_{13} \neq 0$, Phys. Rev. D **93**, 113005 (2016).

[33] T. Fukuyama and H. Nishiura, Mass matrix of Majorana neutrinos, arXiv:hep-ph/9702253.

[34] E. Ma and M. Raidal, Neutrino mass, muon anomalous magnetic moment, and lepton flavor nonconservation, Phys. Rev. Lett. **87**, 011802 (2001); **87**, 159901(E) (2001).

[35] C. S. Lam, A 2-3 symmetry in neutrino oscillations, Phys. Lett. B **507**, 214 (2001).

[36] K. R. S. Balaji, W. Grimus, and T. Schwetz, The solar LMA neutrino oscillation solution in the Zee model, Phys. Lett. B **508**, 301 (2001).

[37] P. F. Harrison and W. G. Scott, μ-τ reflection symmetry in lepton mixing and neutrino oscillations, Phys. Lett. B **547**, 219 (2002).

[38] P. F. Harrison, D. H. Perkins, and W. G. Scott, Tri-bimaximal mixing and the neutrino oscillation data, Phys. Lett. B **530**, 167 (2002).

[39] C. S. Lam, Mass independent textures and symmetry, Phys. Rev. D **74**, 113004 (2006).

[40] P. A. Zyla *et al.* (Particle Data Group), Review of particle physics, Prog. Theor. Exp. Phys. **2020**, 083C01 (2020).

[41] K. collaboration, KATRIN design report 2004, https://www.katrin.kit.edu/publikationen/DesignReport2004-12Jan2005.pdf.

[42] N. Aghanim *et al.* (Planck Collaboration), Planck 2018 results. VI. Cosmological parameters, Astron. Astrophys. **641**, A6 (2020); **652**, C4(E) (2021).

[43] E. Di Valentino *et al.* (CORE Collaboration), Exploring cosmic origins with CORE: Cosmological parameters, J. Cosmol. Astropart. Phys. 04 (2018) 017.

[44] J. Angrik *et al.* (KATRIN Collaboration), KATRIN Design Report 2004, Wissenschaftliche Berichte, FZ Karlsruhe 7090, (2004).

[45] S. Mertens (KATRIN Collaboration), Status of the KATRIN experiment and prospects to search for keV-mass sterile neutrinos in tritium β-decay, Phys. Procedia **61**, 267 (2015).

[46] A. Nucciotti *et al.*, Status of the HOLMES experiment to directly measure the neutrino mass, J. Low Temp. Phys. **193**, 1137 (2018).

[47] A. Ashtari Esfahani *et al.* (Project 8 Collaboration), Determining the neutrino mass with cyclotron radiation emission spectroscopy—Project 8, J. Phys. G **44**, 054004 (2017).

[48] M. Agostini *et al.*, Background-free search for neutrinoless double-β decay of ^{76}Ge with GERDA, Nature (London) **544**, 47 (2017).

[49] J. B. Albert *et al.* (nEXO Collaboration), Sensitivity and discovery potential of nEXO to neutrinoless double beta decay, Phys. Rev. C **97**, 065503 (2018).

[50] D. J. Fixsen, E. S. Cheng, J. M. Gales, J. C. Mather, R. A. Shafer, and E. L. Wright, The cosmic microwave background spectrum from the full COBE FIRAS data set, Astrophys. J. **473**, 576 (1996).

[51] J. Preskill, S. P. Trivedi, F. Wilczek, and M. B. Wise, Cosmology and broken discrete symmetry, Nucl. Phys. **B363**, 207 (1991).

[52] G. R. Dvali, Z. Tavartkiladze, and J. Nanobashvili, Biased discrete symmetry and domain wall problem, Phys. Lett. B **352**, 214 (1995).

[53] B. Holdom, Domain walls. 2. Baryon number generation, Phys. Rev. D **28**, 1419 (1983).

[54] T. Banks and N. Seiberg, Symmetries and strings in field theory and gravity, Phys. Rev. D **83**, 084019 (2011).

[55] D. Harlow and H. Ooguri, Constraints on symmetries from holography, Phys. Rev. Lett. **122**, 191601 (2019).

[56] J. Polchinski, *String Theory. Vol. 2: Superstring Theory and Beyond*, Cambridge Monographs on Mathematical Physics (Cambridge University Press, Cambridge, England, 2007).

[57] A. D. Linde, *Particle Physics and Inflationary Cosmology* (Harwood, Chur, Switzerland, 1990), Vol. 5.

[58] K. A. Olive, Inflation, Phys. Rep. **190**, 307 (1990).

[59] G. R. Dvali and G. Senjanovic, Is there a domain wall problem?, Phys. Rev. Lett. **74**, 5178 (1995).

[60] E. Komatsu *et al.* (WMAP Collaboration), Seven-year Wilkinson microwave anisotropy probe (WMAP) observations: Cosmological interpretation, Astrophys. J. Suppl. Ser. **192**, 18 (2011).

[61] A. Vilenkin, Gravitational field of vacuum domain walls and strings, Phys. Rev. D **23**, 852 (1981).

[62] A. Vilenkin and E. P. S. Shellard, *Cosmic Strings and Other Topological Defects* (Cambridge University Press, Cambridge, England, 2000).

[63] J. Preskill, S. P. Trivedi, F. Wilczek, and M. B. Wise, Cosmology and broken discrete symmetry, Nucl. Phys. **B363**, 207 (1991).

[64] M. Gleiser and R. Roberts, Gravitational waves from collapsing vacuum domains, Phys. Rev. Lett. **81**, 5497 (1998).

[65] T. Hiramatsu, M. Kawasaki, and K. Saikawa, Gravitational waves from collapsing domain walls, J. Cosmol. Astropart. Phys. 05 (2010) 032.

[66] M. Kawasaki and K. Saikawa, Study of gravitational radiation from cosmic domain walls, J. Cosmol. Astropart. Phys. 09 (2011) 008.

[67] T. Hiramatsu, M. Kawasaki, and K. Saikawa, On the estimation of gravitational wave spectrum from cosmic domain walls, J. Cosmol. Astropart. Phys. 02 (2014) 031.

[68] A. M. M. Leite, C. J. A. P. Martins, and E. P. S. Shellard, Accurate calibration of the velocity-dependent one-scale model for domain walls, Phys. Lett. B **718**, 740 (2013).

[69] T. Hiramatsu, M. Kawasaki, K. Saikawa, and T. Sekiguchi, Axion cosmology with long-lived domain walls, J. Cosmol. Astropart. Phys. 01 (2013) 001.

[70] M. Kawasaki, K. Saikawa, and T. Sekiguchi, Axion dark matter from topological defects, Phys. Rev. D **91**, 065014 (2015).

[71] K. Kadota, M. Kawasaki, and K. Saikawa, Gravitational waves from domain walls in the next-to-minimal supersymmetric standard model, J. Cosmol. Astropart. Phys. 10 (2015) 041.